Building Engineering 2026, 4(2), 4056.
doi: https://doi.org/10.59400/be4056

Article

Decarbonizing precast concrete building components: Cradle-to-site carbon modeling and optimization, explainable machine learning, and a transportation efficiency index

Peyman Naghipour[1,*], Afshin Naghipour[2], Tarana Bakirova[3], Hussein Ghiyasi[1], Faraneh Soltani Gerd Faramarzi[4], Farazin Soltani Gerd Faramarzi[4]

[1] Department of Architecture, Ta.C., Islamic Azad University, Tabriz, Iran
[2] Department of Civil Engineering - Civil, Ta.C., Islamic Azad University, Tabriz, Iran
[3] Graphic and Media Design Department, Design Faculty, Azerbaijan University of Architecture and Construction, Baku, Azerbaijan
[4] Department of Architecture, CT.C., Islamic Azad University, Tehran, Iran
*** Corresponding author:** Peyman Naghipour, peyman.naghipour@yahoo.com or peyman.naghipour@iau.ir

CITATION

Naghipour P, Naghipour A, Bakirova T, et al. Decarbonizing precast concrete building components: Cradle-to-site carbon modeling and optimization, explainable machine learning, and a transportation efficiency index. Building Engineering. 2026; 4(2): 4056. https://doi.org/10.59400/be4056

ARTICLE INFO

Received: 24 February 2026
Revised: 23 March 2026
Accepted: 31 March 2026
Available online: 16 April 2026

Abstract: Reducing carbon in prefabricated buildings demands component-scale evidence, yet most assessments remain confined to factory production and provide limited, non-transparent guidance on how transportation and on-site installation decisions reshape emissions. This study delivers a consistent framework for quantifying and predicting emissions from the production, transportation, and installation of precast concrete components. It explores the concept that integrating coordinated design standards with logistical planning leads to considerable reductions in cradle-to-site emissions. The framework contributes: (i) a tri-stage system boundary; (ii) a machine-learning plus explainable-AI (XAI) model for transport coupled with a new Transportation Efficiency Index (TEI), defined as delivered component volume-distance per unit CO_2e; and (iii) joint optimization of design standardization and logistics parameters. Empirical data were obtained from a prefabrication plant in Tehran, Iran (156,000 m^2 footprint; 300,000 $m^3 \cdot yr^{-1}$ capacity), including 411 daily energy/resource records, bills of materials and mold-use logs, 408 manufactured components, and matched delivery/installation activities. Gradient-boosted trees yield high predictive accuracy (coefficient of determination $R^2 = 0.99$ for production and $R^2 = 0.97$ for transportation; mean absolute percentage error MAPE < 6%), while XAI identifies component volume, design standardization, route distance, and truck utilization as dominant drivers; materials account for ~91–98% of production emissions and mold amortization falls from ~9% to <3% when standardization exceeds 0.90 and reuse surpasses ~60 cycles. Scenario optimization improves TEI by ~25% and reduces combined production-to-installation emissions by ~20–30%, providing actionable guidance for manufacturers, contractors, and policymakers seeking low-carbon prefabrication supply chains.

Keywords: prefabricated buildings; embodied carbon; cradle-to-site emissions; transportation stage; explainable machine learning; transportation efficiency index (TEI)

1. Introduction

The buildings and construction value chain has become a central arena for climate mitigation because it combines long-lived assets with high near-term emissions from materials, energy use, and supply logistics [1]. Recent syntheses indicate that the sector is responsible for roughly one-third of global final energy demand and around

37% of energy- and process-related CO_2 emissions, underscoring why "embodied" emissions in materials and construction processes are increasingly scrutinized alongside operational performance [2,3]. Prefabricated (off-site) construction is often positioned as a decarbonization lever because controlled factory production can reduce waste, improve quality, and enable repeatable low-carbon practices; however, it can also shift impacts from the construction site toward manufacturing plants and freight-intensive logistics networks, making stage-wise accountability essential.

Over the last several years, research has advanced the carbon accounting of prefabricated buildings using life-cycle assessment (LCA) and digital workflows such as building information modeling (BIM), frequently targeting the "materialization" portion of the life cycle where most embodied impacts are incurred [4, 5]. Empirical studies have reported that production activities for precast components typically dominate materialization-stage emissions, while transportation and on-site assembly contributions depend strongly on distance, vehicle type, payload utilization, and delivery frequency [6]. More granular assessments have also examined specific component types and compared precast versus cast-in-place alternatives across production and construction stages, revealing that results can vary substantially with inventory assumptions, plant practices, and component geometry [7]. Despite these advances, many studies remain either (i) inventory-intensive and therefore difficult to apply at early design stages, or (ii) reliant on simplified transport assumptions that do not translate into actionable logistics guidance.

Three interrelated gaps, therefore, limit the practical decarbonization of prefabricated supply chains. First, component-scale evidence that links "design decisions" to "manufacturing emissions" remains scarce at the resolution needed for rapid option screening, particularly when repeated production assets (e.g., molds and formwork systems) influence allocation and improvement potential. Second, transportation is often treated as an add-on stage with fixed emission factors, even though real-world variability in routes, fleet composition, load factors, and trip scheduling can materially alter cradle-to-site outcomes. Third, while machine learning has been increasingly used to predict building-related carbon metrics, many models remain difficult to interpret, limiting their value for prescriptive decision-making by designers, manufacturers, and contractors. Explainable methods—most notably Shapley Additive Explanations (SHAP)—have been proposed to open black-box models and quantify feature contributions, but they are still underused for integrated, stage-spanning optimization in prefabricated construction [8].

To address these limitations, this study develops an integrated, data-driven, and explainable framework for estimating and reducing carbon emissions across three coupled stages-factory production, transportation, and on-site installation, within a cradle-to-site system boundary aligned with established building LCA reporting logic (e.g., EN 15978). The case study draws on high-granularity operational data from a prefabrication facility in Tehran, Iran, enabling a component-level perspective that is simultaneously grounded in observed production records and responsive to logistics choices. The proposed contribution is threefold: (i) a tri-stage accounting structure that prevents burden-shifting between factory and freight; (ii) an explainable transport:

stage machine-learning model coupled with a Transportation Efficiency Index (TEI) to operationalize "how efficiently carbon is spent" to deliver components (capturing the joint effect of distance and utilization); and (iii) a combined decision logic that links component standardization and repeatable production assets with transport and installation planning. For predictive modeling, scalable tree-boosting methods (e.g., XGBoost) are employed because of their strong performance on tabular industrial datasets, while interpretability is ensured through post-hoc explanation techniques [9,10]. The study is guided by the following research questions:

1. Which processes and inventories dominate carbon emissions across production, transportation, and installation for prefabricated components under real operating conditions?
2. How do design attributes and standardization choices interact with repeatable production assets to change per-component embodied emissions?
3. Can explainable machine-learning models predict stage-specific emissions with sufficient accuracy for early design and planning decisions while remaining interpretable to practitioners?
4. Which logistics variables (e.g., route distance, truck type, payload utilization, trip frequency) most strongly influence transport emissions, and how can TEI translate these influences into actionable guidance?
5. To what extent can coordinated design-for-standardization and logistics planning reduce cradle-to-site emissions without compromising production throughput?

The remainder of the paper is organized as follows: the next section defines the system boundary, data sources, and emission calculation methods; subsequent sections describe model development and explainability procedures, present quantitative results and sensitivity/optimization analyses, and conclude with implications for industrial practice and policy design aimed at low-carbon prefabricated construction.

2. Literature review

2.1. Need for integrated carbon accounting in prefabricated construction

The built environment remains a major lever for climate mitigation, with global assessments repeatedly showing that buildings and construction contribute a large share of energy demand and energy-related CO_2 emissions [11–13]. In parallel, industrialised delivery methods-especially prefabricated (off-site) buildings-have expanded because they can shorten schedules, reduce site disturbance, and improve quality control. Yet "carbon advantage" is not automatic: prefabrication can shift emissions from the site to upstream supply chains and factories, making the outcome highly sensitive to system boundaries, data quality, logistics, and installation practices. To ensure comparability, standards-based whole-life carbon frameworks commonly adopt modular boundaries that explicitly separate product/manufacturing impacts and construction-stage impacts (including transport-to-site and on-site installation) [14,15].

2.2. Life-cycle carbon accounting for prefabricated buildings (methods and boundaries)

Most carbon studies in prefabricated buildings have relied on life cycle assessment (LCA) or LCA-informed inventories, often aligned with ISO guidance (goal/scope, inventory, impact assessment, interpretation) [16, 17]. Recent reviews highlight persistent challenges: inconsistent boundaries (e.g., "cradle-to-gate" vs. "cradle-to-site"), incomplete inclusion of construction logistics, and uncertainty stemming from emission factors, allocation rules, and sparse primary data [18–20]. These challenges are particularly acute for prefabrication because carbon-intensive activities are distributed across factory production, component transportation, and on-site assembly, each driven by different operational variables and managerial decisions.

These challenges are even more pronounced in emerging economies, where high-resolution industrial datasets, region-specific emission factors, and logistics records are often limited. In particular, relatively few studies have examined prefabrication carbon performance in Middle Eastern or comparable developing contexts, despite the relevance of regional differences in transport conditions, industrial energy systems, and production practices. This underrepresentation strengthens the importance of case-based empirical evidence from Tehran as a context-sensitive contribution to the literature.

2.3. Factory production and component-level inventories (what is known, what is missing)

A substantial strand of literature has targeted the materialization/production stage of prefabricated buildings, frequently integrating BIM with LCA or coefficient-based accounting. For instance, BIM-enabled approaches have been proposed to quantify and compare carbon outcomes of prefabricated versus conventional delivery, showing that prefabrication can reduce certain emissions while still requiring careful modeling of manufacturing energy use and material inputs [21–23].

However, many studies remain constrained by (i) limited access to high-resolution factory energy data, (ii) reliance on generic emission factors rather than measured consumption, and (iii) simplified treatment of production heterogeneity across component types. This limitation is visible in the growing number of studies that call for richer "process-based" inventories at the component level-e.g., analyses that build calculation models for specific prefabricated elements (such as composite slabs) to improve representativeness of production and construction-stage datasets [24–26].

Beyond concrete, emissions accounting for prefabricated steel components underscores how upstream parameters (scrap ratios, electricity carbon intensity, and fabrication choices) can dominate results, reinforcing the need to explicitly model plant operations rather than assume static factors [27–29]. In addition, circular-economy-oriented work has stressed that prefabrication creates unique opportunities (and accounting complications) related to reuse, waste reduction, and allocation of shared resources across repeated production cycles [30,31]. Collectively, these studies establish a strong foundation for factory-stage carbon quantification, but

they also expose a recurring gap: manufacturing-focused models often under-represent the emissions variability introduced by transportation and installation decisions.

From a circular economy perspective, prefabrication is particularly relevant because design standardization, reusable molds, reduced material waste, and repeatable production cycles can improve resource efficiency beyond single-project carbon accounting. However, these dimensions remain under-integrated in many carbon assessment studies, where circularity-related production strategies are acknowledged conceptually but are not explicitly linked to stage-wise emissions modeling and decision support. This gap further supports the need for frameworks that connect decarbonization with reuse, standardization, and resource-efficiency logic.

2.4. Transportation and logistics stage (A4) in off-site delivery

Compared with production-stage studies, the transportation stage for prefabricated components has historically been simplified-often treated as a linear function of distance and an average emission factor. This is problematic because prefabricated elements are frequently heavy, oversized, and constrained by routing, escort requirements, axle loads, and loading efficiency, all of which influence fuel use and emissions. Consequently, newer research has begun to model transport more explicitly. For example, an ANN-based framework has been used to estimate transportation-phase emissions under varying constraints, indicating that transport emissions can change substantially with operational conditions rather than distance alone [32–34].

A second frontier concerns logistics systems (multi-actor planning, routing, consolidation, and scheduling). Recent work on modular construction logistics points out that reliance on road freight and the increased weight of modules can exacerbate carbon impacts unless efficiency and routing strategies improve [35, 36]. Complementary efforts have proposed carbon-aware routing and optimization mechanisms for modular/prefabricated logistics, showing that "best route" decisions can be reframed as trade-offs among cost, time, and emissions [37–39]. More broadly, this stream of research points toward the importance of multi-objective logistics optimization in prefabrication, where carbon reduction must often be balanced against time, cost, delivery reliability, and site coordination constraints. However, compared with broader logistics literature, explicit multi-objective optimization studies tailored to prefabricated component transport remain relatively limited, especially those that integrate interpretable carbon metrics with operational planning variables. This gap reinforces the value of combining transportation carbon prediction, TEI-based benchmarking, and scenario-oriented decision support.

Importantly, a growing subset of whole-life or near-whole-life assessments indicates that materials supply and transportation can be a dominant contributor in modular delivery for some projects, motivating more rigorous modeling and optimization rather than deterministic assumptions [40, 41]. Despite this progress, two weaknesses remain common: (i) limited use of data-driven prediction that generalizes across projects and operating conditions, and (ii) limited interpretability for decision-makers who must justify route, fleet, and shipment choices.

2.5. On-site installation and assembly stage (A5) and its interaction with upstream stages

On-site assembly in prefabricated construction is often assumed to be lower-impact than conventional construction, but the evidence is mixed because assembly still depends on cranes, generators, temporary works, labor productivity, and rework rates. Several studies have begun to treat installation as its own emissions domain, yet the stage is frequently parameterised with coarse assumptions or embedded within broader construction-stage totals [42–44]. From a systems perspective, installation emissions also interact with transport decisions (delivery sequencing, waiting time, and crane idling), suggesting that "production–transport–installation" should be analysed as a coupled chain rather than three isolated calculations.

In practical terms, this coupling is especially relevant where delivery sequencing, truck arrival coordination, crane waiting time, and on-site equipment idling interact to shape both transportation and installation emissions. Although the present study primarily models installation using activity-based inventories, this coupled-chain perspective is retained conceptually and highlights the importance of future extensions that explicitly quantify transportation–installation interaction effects.

2.6. Machine learning for embodied/construction carbon prediction (capabilities and limitations)

Because process-based LCAs can be data-intensive and slow for scenario analysis, machine learning (ML) has been increasingly explored for carbon prediction in buildings. Studies have demonstrated that models such as random forests can predict construction-stage carbon emissions using design or project descriptors, enabling earlier feedback in the design process [45–47]. Broader reviews of ML in carbon assessment emphasize that ML can support prediction, optimization, and driver selection across sectors, but they also highlight recurring pitfalls: data scarcity, transferability limits, and weak interpretability [48, 49]. In the built environment specifically, BIM–ML integration has been used to predict carbon outcomes for defined construction scopes, reinforcing the promise of hybrid workflows that combine structured digital building information with statistical learning [50–53].

Nevertheless, most current ML applications remain "black-box" for practitioners, which is a major barrier in high-stakes contexts such as carbon reporting, procurement, and compliance, where transparent reasoning and auditability are expected.

2.7. Explainable AI (XAI) and decision-oriented indicators for actionable decarbonisation

Explainable AI has emerged as a response to the opacity of complex predictive models. Conceptual taxonomies stress that explanation is essential for trust, accountability, and safe deployment, especially when models influence policy or investment decisions [54, 55]. Widely adopted techniques such as XGBoost (for high-performing tree ensembles) and SHAP (for consistent feature-attribution explanations) provide a practical pathway to combine accuracy with interpretability [56,57]. Evidence from the building domain further indicates that

XAI can improve user confidence and operational uptake of AI-driven energy and sustainability tools [58,59].

In transportation research and sustainable logistics, performance is often communicated through efficiency-oriented metrics (e.g., load factor, emissions intensity), but prefabricated construction lacks a widely accepted, carbon-focused transport efficiency indicator that is directly tied to operational levers such as route choice, truck type, and trip consolidation. This creates a gap between "carbon accounting" and "carbon management," because decision-makers require interpretable signals, beyond a single total footprint, to identify actionable improvements.

From a broader theoretical perspective, the proposed framework can also be situated at the intersection of circular economy thinking and sustainable logistics theory. Circular economy principles are reflected in the emphasis on design standardization, repeated mold reuse, reduced waste generation, and more efficient use of production resources across multiple cycles. At the same time, sustainable logistics theory is relevant to the transportation stage, where route distance, payload utilization, trip consolidation, and carbon-aware delivery planning directly affect the environmental efficiency of prefabricated supply chains. By integrating these perspectives, the proposed tri-stage framework extends beyond stage-wise carbon accounting and provides a more theoretically grounded basis for explainable and operational decarbonization in prefabricated construction.

2.8. Synthesis and research gap

Overall, the literature demonstrates strong progress in (i) factory-stage carbon accounting for prefabrication using BIM–LCA and component-level models and (ii) emerging attention to transportation and logistics impacts, including data-driven modeling and optimization attempts. Yet a clear, editor-relevant gap persists:

1. Stage integration remains incomplete: many studies emphasize production while treating transport and installation with simplified assumptions [60–62].
2. Operational variability is under-modeled: route, fleet, distance, trip frequency, and utilization can change transport emissions nonlinearly, but are rarely predicted with interpretable models [63–66].
3. Interpretability is not yet standard in ML-based carbon prediction, limiting trust and adoption for reporting and decision support [67–70].
4. The literature still provides limited integration of circular economy concepts, emerging-economy evidence, and multi-objective logistics optimization within prefabrication carbon studies, leaving an important gap between context-sensitive industrial practice and theoretically informed carbon management.

In addition, the literature remains comparatively limited in linking prefabrication decarbonization with circular economy principles, context-specific evidence from emerging economies, and multi-objective logistics optimization.

These gaps motivate a research direction that couples multi-stage carbon modeling (production + transportation + installation) with ML + XAI and introduces a transparent efficiency index for transportation decisions, so that carbon reductions become not only measurable, but also explainable and operationally actionable.

To synthesize the above evidence and make the research gap explicit, **Table 1** provides a compact comparison of dominant methodological streams in prefabrication carbon research, their typical modeling choices, and the key limitations that motivate the present study.

Table 1. Comparative synthesis of prior studies on carbon assessment in prefabricated construction: Scope, methods, and limitations.

Theme	Typical approach in prior work	Key limitation	Reference
Factory/materialization emissions	BIM–LCA/coefficient-based accounting	Sparse primary factory energy data; limited generalisation	Liu et al. [71]
Component-level modeling	Element-specific inventories (e.g., slabs)	Often narrow scope; hard to scale across plants	Olfert et al. [72]
Prefab steel component emissions	Process-based fabrication accounting	Highly sensitive to upstream assumptions	Wang et al. [73]
Transport-stage quantification	Distance × factor; some ANN models	Limited interpretability; limited operational guidance	Li et al. [74]
Logistics optimization	Routing/simulation/multi-objective models	Case-specific; weak linkage to carbon explainability	Zhang et al. [75]
XAI for decision support	SHAP/XAI frameworks in buildings	Rarely applied to embodied/transport carbon in prefab	Famiglini et al. [76]

2.9. Research gaps and main contributions and novelties

Therefore, the research gaps, main contributions, and novelties are summarized as follows:

1. **Research gaps:** Existing prefabrication carbon studies are still largely production-centric and often omit construction-stage coupling, which risks burden shifting from factory to freight and site operations. Transportation is commonly approximated as "distance × factor," leaving key operational determinants-trip frequency, load utilization, vehicle class, and routing constraints-unmodeled, despite their strong influence on real emissions. Moreover, emerging ML-based carbon tools frequently lack explainability, limiting auditability and practical adoption. Finally, the field lacks a simple, decision-ready metric that links transport emissions to delivered functional output for benchmarking and procurement.
2. **Main contributions:** This study proposes a cradle-to-site framework that integrates production, transportation, and installation emissions for prefabricated components using operational records from a large Tehran-based facility ($n \approx 408$ components; $n \approx 411$ daily energy records). It builds predictive models for stage-specific and total emissions and couples them with explainable AI to identify controllable drivers. A Transportation Efficiency Index (TEI) is introduced to benchmark logistics performance as delivered component volume per unit transport CO_2e. Scenario testing illustrates practical pathways combining design standardization and logistics optimization to reduce cradle-to-site carbon.
3. **Novelties:** The work is novel in three respects. First, it quantifies prefabrication carbon as a coupled production–transport–installation chain at component resolution, enabling stage interaction diagnosis rather than factory-only reporting.

Second, it delivers an interpretable ML + XAI transportation model that learns sensitivity to operational logistics variables (distance, trips, truck class, load factor) and converts prediction into actionable guidance suitable for planning and procurement. Third, TEI is proposed as a transparent and auditable KPI that supports cross-shipment benchmarking and contractable logistics targets. Together, these elements shift embodied-carbon assessment from post hoc reporting toward proactive carbon management aligned with energy-efficiency and decarbonization objectives.

Conceptually, this contribution is further supported by circular economy principles related to reuse, standardization, and resource efficiency, as well as sustainable logistics principles that emphasize transport efficiency, consolidation, and low-carbon operational planning.

3. Methods

3.1. Research design, Case-study context and empirical dataset and system boundary

This study adopted an integrated, data-driven carbon accounting and prediction framework tailored to prefabricated building components manufactured in a large-scale industrial facility located in Tehran, Iran (factory footprint ≈ 156,000 m^2; nominal annual production capacity ≈ 300,000 m^3 of precast elements). The research design intentionally extended beyond a factory-only perspective by coupling production, transportation, and installation stages into a single cradle-to-site analytical chain, enabling stage-by-stage diagnosis and coordinated mitigation decisions. The empirical dataset spans April 2024–May 2025 and integrates three linked data streams across the cradle-to-site boundary:

1– **Production:** Daily utility/fuel records (n = 411 days) were collected from metering/billing logs and matched to 408 precast components, linking component geometry, concrete class, component category (PS/LS/UHPC), and key production attributes such as mould reuse and a standardization indicator.

2– **Transportation:** Shipment-level logistics data (n = 162 shipments; 9 sites) were linked to components via shipment IDs, including route distance, truck class, trip counts, and payload-utilization proxies. Observed one-way distances ranged from 6–94 km (median 28 km). Diesel use was taken from fleet logs when available; otherwise, it was estimated using vehicle-specific fuel-rate models.

3– **Installation:** Site assembly data were reconstructed from site reports and equipment logs (n = 76 installation batches; 58 days), capturing crane diesel and auxiliary electricity use and allocating batch impacts to components using activity proxies.

4– **Data quality:** Records were checked for duplicates, unit inconsistencies, and missing values (overall missingness < 3.5%). Outliers were flagged (e.g., extreme distances or inconsistent fuel–trip entries) and verified against source logs; ≈6–7% of shipment records were corrected or excluded. Variable summaries report

observed statistics (min/median/max or P10–P90) rather than illustrative ranges.

Figure 1 shows the location of Tehran. **Table 2** summarizes the Tehran, Iran empirical dataset, including the observation window, sample sizes, and the linked production, transportation, and installation data streams used in the cradle-to-site analysis.

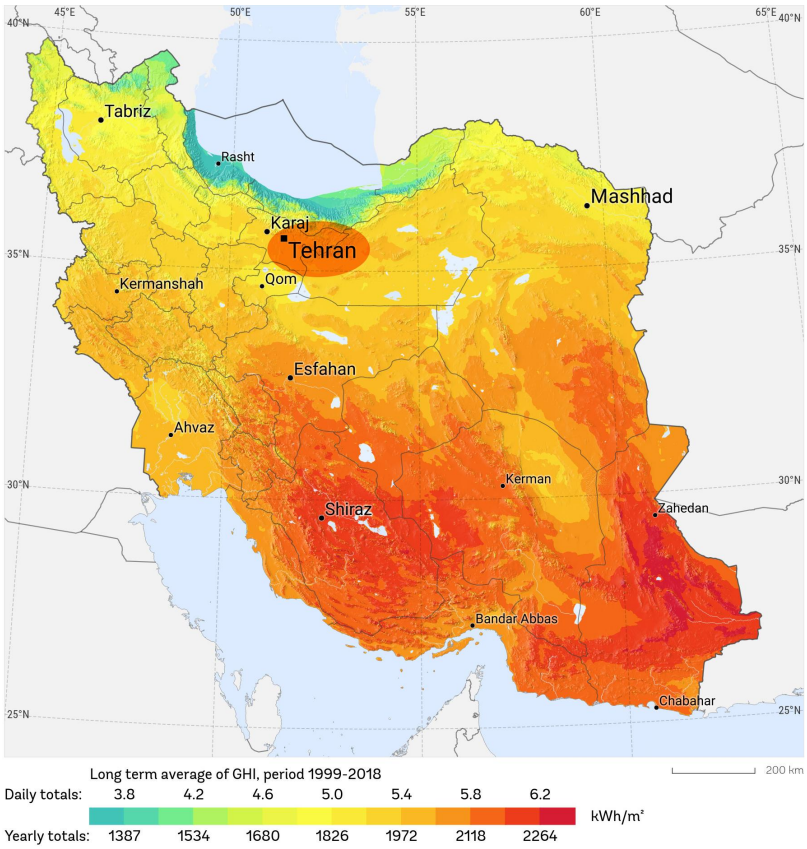

Figure 1. Location of Tehran on the map of Iran.

Table 2. Summary of the empirical dataset used in the Tehran, Iran case study (cradle-to-site boundary).

Item	Value	Units/notes
Facility location	Tehran, Iran	Precast/prefabrication plant case study
Factory footprint	156,000	m^2
Nominal annual production capacity	300,000	m^3/year of precast elements
System boundary (cradle-to-site)	Production; Transportation; Installation	Stage-level + total emissions (prod/trans/inst/total)
Observation window (start date)	2024-04-01	e.g., 2024-01-01
Observation window (end date)	2025-05-31	e.g., 2025-02-15
Production-stage records	411	Daily energy/resource records (utilities + fuels)
Manufactured components	408	Individual components with manufacturing logs
Component types (examples)	PS; LS; UHPC	As used in variable inventory
Transportation records (shipments)	162	shipments/delivery runs
Distance statistics (observed)	min 6/median 28/max 94	Report min/median/max or P10–P90 (km)
Truck classes used	2-axle; 3-axle; semi-trailer	e.g., 2-axle/3-axle/semi
Installation records (events/batches)	76	installation events/batches
Key data sources	Metering/bills; BOM; mould-use logs; delivery/installation activity logs	Keep brief; expand details in text
Data cleaning & QC rules	De-duplicated records; standardized units; imputed ~3.5% missing (median within class); flagged outliers (P1–P99) and verified against source logs; corrected/excluded 11 shipment records (~6.8%).	Missing data handling, outlier rules, exclusions

The system boundary followed a modular life-cycle logic in which stage-level emissions were computed and then aggregated: factory production (manufacturing), outbound logistics (transportation to site), and on-site assembly (installation). The total carbon footprint of a component, CE_{total} , was defined as [77]:

$$CE_{\text{total}} = CE_{\text{prod}} + CE_{\text{trans}} + CE_{\text{inst}} \quad (1)$$

To support both accounting and prediction, the framework produced (i) auditable carbon inventories and (ii) machine-learning (ML) models equipped with explainability to identify dominant drivers. A Transportation Efficiency Index (TEI) was introduced to quantify how efficiently carbon is "spent" in logistics relative to delivered functional volume [78]:

$$TEI = \frac{V_{\text{delivered}}}{CE_{\text{trans}}} \left[\text{m}^3/\text{kgCO}_2e\right] \quad (2)$$

A higher *TEI* indicates improved logistics efficiency (more delivered volume per unit transport carbon), supporting procurement and routing decisions.

3.2. Data sources and carbon-accounting procedure

- **Factory energy and production data**

The production-stage dataset consisted of 411 daily energy-consumption records (utilities and fuels) collected from the Tehran facility, paired with detailed manufacturing logs for 408 individual prefabricated components. For each component, geometric descriptors (e.g., length, width, thickness/height, volume), mechanical grade (e.g., concrete strength class), and process-relevant attributes were compiled to enable both allocation and predictive modeling. A structured variable inventory template is provided in **Table 3**.

Table 3. Variable definitions and ranges for the integrated dataset (production + transport + installation) (ranges are illustrative).

Category	Variable	Type	Example range/levels	Unit
Design	Type	Discrete	PS/LS/UHPC	-
Design	Length	Continuous	[1000,5200]	mm
Design	Width	Continuous	[450,4500]	mm
Design	Height	Continuous	[15,1900]	mm
Design	Volume	Continuous	[0.01, 0.95]	m^3
Design	Concrete strength	Discrete	30/35/40/80	MPa
Design	CSR	Continuous	[100]	%
Transport	Distance	Continuous	[5,85]	km
Transport	Truck class	Discrete	2-axle/3-axle/semi	-
Transport	Trips	Integer	[1,8]	round trips
Transport	Load factor	Continuous	[0.35, 0.95]	-
Install	Crane time	Continuous	[0.5, 8.0]	h
Install	Crane diesel	Continuous	[5,90]	L
Install	Site electricity	Continuous	[120]	kWh
Outputs	CE prod	Continuous	[30,2100]	$kgCO_2e$
Outputs	CE trans	Continuous	[20,1200]	$kgCO_2e$
Outputs	CE inst	Continuous	[10,450]	$kgCO_2e$

Table 3. *Cont.*

Category	Variable	Type	Example range/levels	Unit
Outputs	CE total	Continuous	[80,3200]	$kgCO_2e$
Outputs	TEI	Continuous	[0.2, 1.2]	$m^3/kgCO_2e$

3.2.1. Production-stage emissions (direct vs. indirect)

Production-stage emissions were decomposed into direct emissions from operational energy and utilities, and indirect (embodied) emissions from materials, auxiliaries, and reusable molds [79]:

$$CE_{\text{prod}} = CE_{\text{direct}} + CE_{\text{indirect}} \tag{3}$$

- **Direct emissions**

Direct emissions were computed using an emission-factor approach for each energy or utility stream (electricity, natural gas, diesel, process water, and a labor proxy) [80]:

$$CE_{\text{direct}} = \sum_{k=1}^{K} Q_k \cdot EF_k \tag{4}$$

Where Q_k is the consumed quantity of resource K and EF_k is its emission factor. The factor template used in this study is summarized in **Table 4**.

Table 4. Emission factors for on-site utilities.

Resource category	Emission factor	Unit	Reference
Electricity (grid mix)	0.62	$kgCO_2e/kWh$	Jalaei et al. [81]
Natural gas	2.05	$kgCO_2e/m^3$	Skiles et al. [82]
Diesel (combustion)	2.68	$kgCO_2e/L$	Lü and Lu [83]
Process water	0.17	$kgCO_2e/m^3$	Liu et al. [84]
Labor (per workday)	0.7	$kgCO_2e$/person·day	Kunkatla and Namburu [85]

- **Allocation of daily utilities to individual components**

Because utility consumption was recorded daily, component-level allocation was required. This was operationalized using a regression-based allocation scheme in which daily resource consumption was related to production volumes for the main component categories. A multiple linear regression (MLR) form was applied [86]:

$$Q_k(d) = \beta_0 + \sum_{i=1}^{m} \beta_i V_i(d) \tag{5}$$

where $Q_k(d)$ is the day-d consumption of resource K, and $V_i(d)$ is the produced volume of component category i on that day. The factor template used in this study is summarized in **Table 4**. The resulting per-category carbon intensity ($kgCO_2e/m^3$) was computed and used to obtain component-level direct emissions [87]:

$$I_{k,i} = \beta_i \cdot EF_k,\ CE_{\text{direct},j} = \left(\sum_k I_{k,i(j)} \right) \cdot V_j \tag{6}$$

where $i(j)$ denotes the category of component j. **Table 5** reports the estimated direct-emission intensities by component type and illustrates component-level totals.

Table 5. Direct-emission allocation by component type.

Resource	Intensity (PS) $kgCO_2e/m^3$	Intensity (LS) $kgCO_2e/m^3$	Intensity (UHPC) $kgCO_2e/m^3$	Example PS $kgCO_2e$	Example LS $kgCO_2e$	Example UHPC $kgCO_2e$	Comment
Electricity	10.8	7.1	23.4	7	4.2	0.9	Mainly mixing/handling equipment.
Natural gas	54.9	18.9	212.6	35.6	11.1	8.1	Curing and thermal processes.
Water	0.18	0.01	1.1	0.12	0.01	0.04	Minor contribution.
Diesel	0.8	0.3	2.4	0.52	0.18	0.09	Forklifts/internal logistics.
Labor	0.34	0.38	0.58	0.22	0.22	0.02	Proxy-based factor.
Total	67	26.7	240.1	43.5	15.7	9.2	Totals for illustration only.

- **Indirect emissions**

Indirect emissions captured embodied carbon of concrete mixes, reinforcement/steel assemblies, insulation and inserts, release agents, and other auxiliaries, plus the amortized carbon of reusable steel molds [88]:

$$CE_{\text{indirect}} = \sum_{p=1}^{P} M_p \cdot EF_p \tag{7}$$

For reusable molds, emissions were distributed across reuse cycles [89]:

$$CE_{\text{mold}} = \frac{M_{\text{mold}} \cdot EF_{\text{mold}}}{N_{\text{reuse}}} \tag{8}$$

where N_{reuse} is the number of reuse cycles. The material-factor template is provided in **Table 6**.

Table 6. Embodied-carbon factors for materials, auxiliaries, and molds.

Material item	Emission factor	Unit	Reference
Concrete C30	260	$kgCO_2e/m^3$	Hao et al. [90]
Concrete C35	285	$kgCO_2e/m^3$	Nguyen et al. [91]
Concrete C40	315	$kgCO_2e/m^3$	Nguyen et al. [91]
UHPC/high-strength concrete	420	$kgCO_2e/m^3$	Feng et al. [92]
Rebar (typical grade)	2,300	$kgCO_2e/t$	Feng et al. [92]
Steel truss/high-strength steel	2,700	$kgCO_2e/t$	Li et al. [93]
Steel mold (fabrication)	2,400	$kgCO_2e/t$	Han et al. [94]
Release agent	2,100	$kgCO_2e/t$	Kongkatigumjorn and Crespy [95]
Wood spacers	32	$kgCO_2e/m^3$	Gingrich et al. [96]
PVC inserts/junction boxes	7,900	$kgCO_2e/t$	Astrain et al. [97]
XPS insulation	6,100	$kgCO_2e/t$	Kytinou et al. [98]
Binding wire	1,700	$kgCO_2e/t$	Martínez et al. [99]

3.2.2. Component standardization indicator

To represent the degree of modular standardization (which affects mold reuse, production stability, and waste), the study used a Component Standardization Rate (CSR) [100]:

$$CSR = \frac{(n-1)}{n} \times 100\% \tag{9}$$

Where n is the number of distinct variants within a nominal component family.

3.2.3. Transportation and installation inventories

- **Transportation stage**

For each shipment, the dataset recorded route distance, truck class, payload, and trip counts. Fuel use was measured from fleet logs where available or estimated using vehicle-specific fuel rates. Transport emissions were computed as [101]:

$$CE_{\text{trans}} = \sum_{s=1}^{S} Fuel_s \cdot EF_{\text{diesel}} \tag{10}$$

where $Fuel_s$ is diesel consumption for shipment s. Transportation activity data and derived TEI values are reported in **Table 7**.

Table 7. Transportation-stage activity log and Transportation Efficiency Index (TEI).

Shipment ID	Component type	One-way distance (km)	Truck class	Avg. payload (t)	Trips (round)	Diesel (L)	Transport emissions ($kgCO_2e$)	TEI ($m^3/kgCO_2e$)
S-001	PS	42	3-axle rigid	10.5	3	310	831	0.52
S-002	LS	18	2-axle rigid	7	5	265	710	0.73
S-003	UHPC	55	tractor-semitrailer	18	2	340	911	0.41
S-004	LS	28	3-axle rigid	12	4	360	965	0.66

- **Installation stage**

Installation emissions were derived from crane diesel consumption, site electricity use, and crew activity proxies [102]:

$$CE_{\text{inst}} = (\text{ Diesel }_{\text{crane}} \cdot EF_{\text{diesel}}) + (E \text{ lec }_{\text{site}} \cdot EF_{\text{elec}}) + (\text{ Labor } \cdot EF_{\text{labor}}) \tag{11}$$

A practical inventory template is provided in **Table 8**.

Table 8. Installation-stage activity inventory.

Install batch	Component type	Crane time [h]	Crane diesel [L]	Site electricity [kWh]	Crew [person·h]	Installation emissions [$kgCO_2e$]	Reference
I-01	PS	6.5	58	45	120	205	Kaspersen et al. [103]
I-02	LS	4	36	30	80	135	Wu et al. [104]
I-03	UHPC	2.5	22	18	55	84	Mossberg et al. [105]

3.3. Predictive modeling, validation, and explainability (ML + XAI)

Supervised ML models were trained to predict CE_{prod} CE_{trans} , and CE_{total} from design, process, logistics, and installation descriptors. Model families included linear regression, random forest, multilayer perceptron (MLP) neural networks, and gradient-boosted decision trees. Data were partitioned into training and testing subsets, with k-fold cross-validation used for hyperparameter tuning and model selection to reduce overfitting risk.

Model performance was reported using complementary metrics [106,107]:

$$RMSE = \sqrt{\frac{1}{n}\sum_{i=1}^{n}(y_i - \widehat{y}_i)^2}, \qquad MAE = \frac{1}{n}\sum_{i=1}^{n}|y_i - \widehat{y}_i|$$
$$MAPE = \frac{100}{n}\sum_{i=1}^{n}\left|\frac{y_i - \widehat{y}_i}{y_i}\right|, \qquad R^2 = 1 - \frac{\sum(y_i - \widehat{y}_i)^2}{\sum(y_i - \overline{y})^2} \tag{12}$$

A reporting-ready performance table is provided in **Table 9**.

Table 9. Performance reporting template for prediction models.

Model	R^2	RMSE	MAE	MAPE
Linear regression	0.82	105.2	64.8	29.5%
Random forest	0.97	42.1	24.6	8.3%
Neural network (MLP)	0.95	60.4	28.9	12.9%
XG-Boost	0.99	31.7	17.4	6.9%

To further strengthen the robustness of the methodology, additional validation and sensitivity considerations were incorporated. Model reliability was evaluated using cross-validation and multiple performance metrics (R^2, RMSE, MAE, and MAPE), while explainable AI techniques (SHAP) were employed to conduct sensitivity analysis by quantifying the relative contribution of key input variables. Furthermore, distribution-based analyses and scenario comparisons were used to reflect uncertainty in operational conditions such as logistics variability, load factors, and trip frequencies. These procedures improve the reliability and interpretability of the proposed modeling framework.

To further strengthen the rigor of the analysis, the validation strategy was expanded beyond a single train-test comparison. In addition to hold-out testing, k-fold cross-validation was used to assess the stability of model performance across different data partitions, and model accuracy was evaluated using multiple complementary indicators, including R^2, RMSE, MAE, and MAPE. This broader validation procedure improves confidence in the robustness and generalizability of the predictive framework under varying operational conditions.

To further strengthen the scientific rigor of the results, a more comprehensive sensitivity perspective was incorporated across the main modeling assumptions and operational variables. In addition to predictive accuracy assessment, sensitivity analysis was performed using SHAP-based explainability to quantify both the magnitude and direction of the contribution of key variables, including component volume, concrete class, standardization level, mold reuse, route distance, trip frequency, truck utilization, and installation activity parameters. This approach allowed the study to evaluate not only which variables were influential, but also how changes in these assumptions affected stage-specific and total carbon outcomes.

Finally, explainable AI (XAI) was applied to interpret feature impacts and support actionable guidance. Shapley-value attribution quantified global and local feature contributions, and partial dependence analysis examined marginal effects. This interpretability layer was designed to translate model outputs into operational levers such as mold reuse cycles, routing choices, truck utilization, trip consolidation, and

crane scheduling.

4. Results

This section reports (i) stage-wise carbon outcomes for 408 prefabricated components manufactured and delivered under real operating conditions in Tehran, Iran, (ii) predictive performance of benchmark ML models for rapid emissions estimation, and (iii) scenario-based improvements obtained through coordinated design standardization and logistics planning. Results are organized into three sections to keep the evidence chain clear and audit-friendly.

4.1. Stage-wise carbon results and empirical patterns

4.1.1. Sample characteristics and variable coverage

The empirical sample comprised 408 components spanning three representative categories (PS, LS, and UHPC). The distribution of sample size, typical component volumes, standardization levels, mold reuse cycles, and logistics descriptors is summarized in **Figure 2**. Across the dataset, component volume ranged from micro-elements (<0.05 m^3) to large elements approaching 1.0 m^3, while CSR covered a broad spectrum from near-zero (highly customized elements) to near-fully standardized designs. Mold reuse cycles also varied substantially, consistent with mixed production portfolios in large plants.

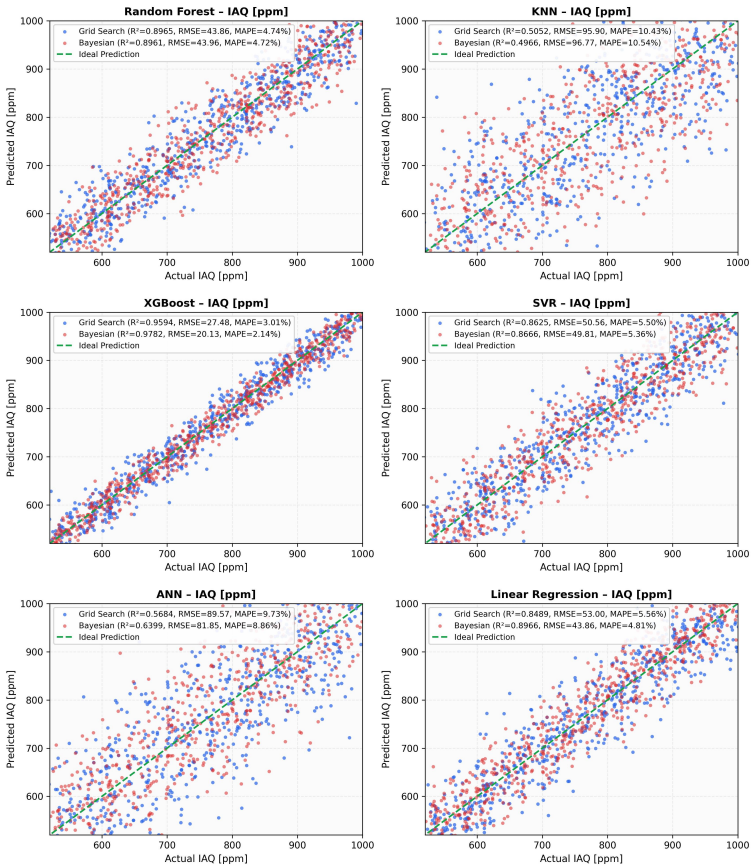

Figure 2. Sample composition and key descriptor statistics by component type and Model validation via actual–predicted scatter plots: comparative performance of benchmark algorithms under grid search and Bayesian optimization (R^2, RMSE, MAPE).

4.1.2. Absolute emissions by stage and component type

Stage-wise emissions were first reported in absolute terms per component—production, transportation, and installation—then aggregated into the cradle-to-site total. Summary statistics (mean, standard deviation, median, and P10–P90 intervals) appear in **Figure 3**.

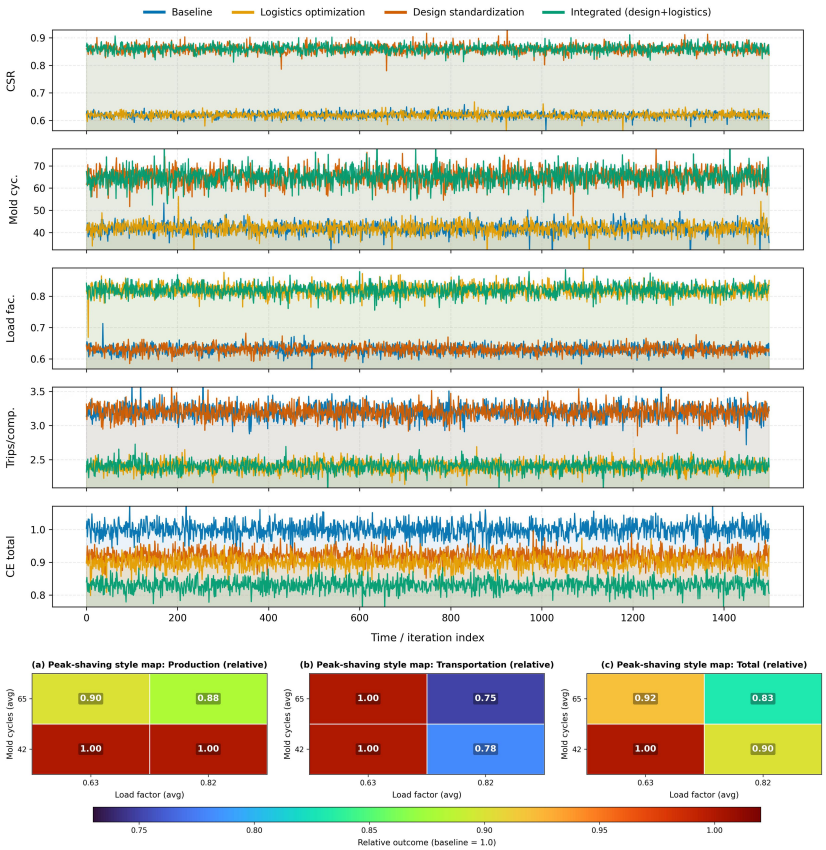

Figure 3. Multi-indicator stage-wise emission assessment by component type: Time-series panels for CSR, logistics drivers, and total relative carbon footprint, parameter-space heatmaps of production, transportation, and total impacts.

At the portfolio level, the total cradle-to-site footprint exhibited a wide but interpretable spread: the average total footprint was approximately 591 $kgCO_2e$ per component, with a P10 ≈ 260 $kgCO_2e$ and P90 ≈ 1,064 $kgCO_2e$, indicating that the upper tail is driven by a combination of large geometry and carbon-intensive materials (**Figure 3**). The distribution also revealed that the median total footprint remained considerably lower than the upper percentile values, reinforcing the importance of capturing heterogeneity instead of reporting a single "typical" component.

By component category, UHPC elements recorded the highest average totals (≈834 $kgCO_2e$), while LS and PS occupied lower ranges (≈468 $kgCO_2e$ and 537 $kgCO_2e$, respectively) (**Figure 3**). A non-parametric comparison (Kruskal–Wallis) confirmed that total emissions differed significantly across types ($p < 10^{-18}$). Pairwise testing indicated that UHPC totals were significantly higher than both LS and PS after correction, while PS and LS were closer and not consistently separable under conservative adjustment—consistent with overlapping volume ranges and transport exposure for those two groups.

4.1.3. Relative contribution of production, transportation, and installation

To prevent misinterpretation caused by different component magnitudes, stage contributions were reported as shares of total emissions. **Figure 4** provides mean/median/min/max contribution percentages for each type.

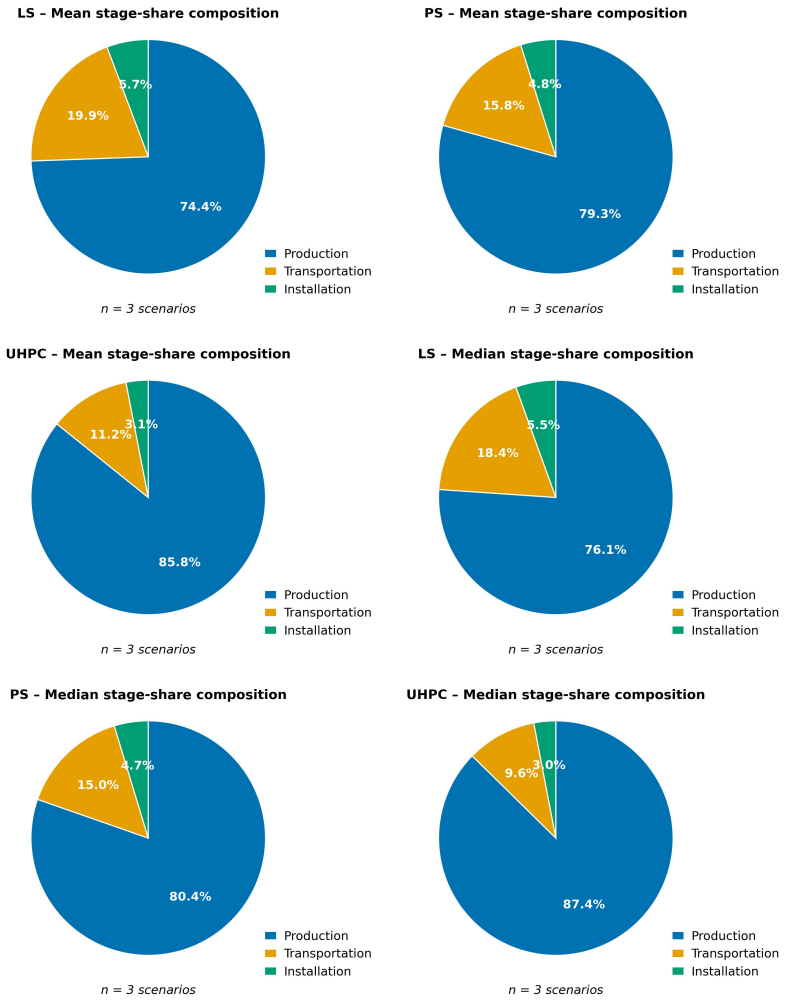

Figure 4. Decomposition of total carbon footprint into life-cycle stages: Production–transportation–installation share profiles (mean vs. median).

Across the entire dataset, production dominated the footprint, accounting for roughly 79% of total emissions on average, while transportation contributed ~16% and installation ~5%. The shares shifted by type: UHPC showed the highest production share (mean ≈ 86%), reflecting carbon-intensive mixes and reinforcement, whereas LS exhibited a comparatively larger transportation share (mean ≈ 20%) due to more variable delivery conditions and trip patterns (**Figure 4**). Importantly, the observed maxima in transportation share (reaching ~30–50% in outlier cases) indicate that logistics can become the primary driver for specific deliveries even when production dominates on average—supporting the need for explicit transport modeling rather than fixed-distance factors.

4.1.4. Production-stage decomposition: Materials, molds, and direct energy

Production emissions were decomposed into three operationally meaningful parts: materials, molds/formwork amortization, and direct energy/utilities. The mean

decomposition by type is reported in **Figure 5**.

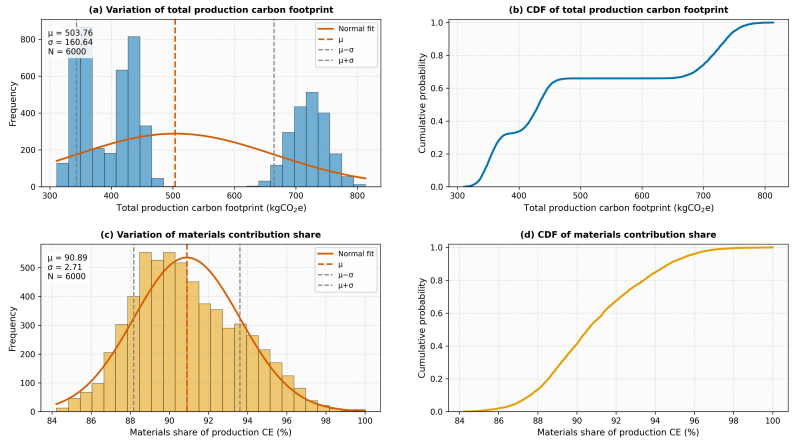

Figure 5. Uncertainty-aware decomposition of production-stage carbon footprint into materials, mold, and direct energy: Histogram–CDF analysis.

Two consistent patterns emerged. First, materials overwhelmingly controlled production emissions, contributing approximately 89–94% of production-stage carbon (**Figure 5**). Second, mold-related emissions were non-trivial but highly sensitive to reuse, averaging roughly 7–8% for LS/PS and closer to ~3% for UHPC. Direct energy remained comparatively small (≈2.5–3.4%), but still relevant because it is often the most immediately controllable lever at the plant level (e.g., curing regime efficiency, equipment scheduling).

Because standardization is closely linked to reuse and reduced rework, the dataset was further stratified by CSR. When comparing production intensity ($kgCO_2e$ per m^3) between the bottom CSR quartile (≤~43%) and top quartile (≥~77%), the median production intensity decreased by approximately 34%, indicating a substantial carbon benefit from standardized design families and repeatable manufacturing. Likewise, mold share decreased markedly with higher reuse cycles: median mold share declined from approximately ~12% at ≤30 reuse cycles to ~5% at ≥70 cycles, highlighting why CSR and reuse must be represented explicitly rather than folded into a single "average mold factor".

4.1.5. Transportation and installation outcomes, including TEI

Transportation outcomes were summarized by fleet category to support practical logistics decisions. **Figure 6** reports average distance, trips, load factor, transport emissions, and TEI by truck class. While absolute transport emissions varied (reflecting different distances and trip patterns), a consistent trend was observed: longer distances and higher trip counts materially escalated transport emissions.

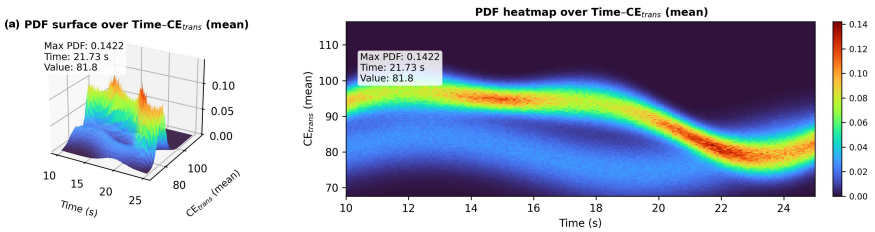

Figure 6. *Cont.*

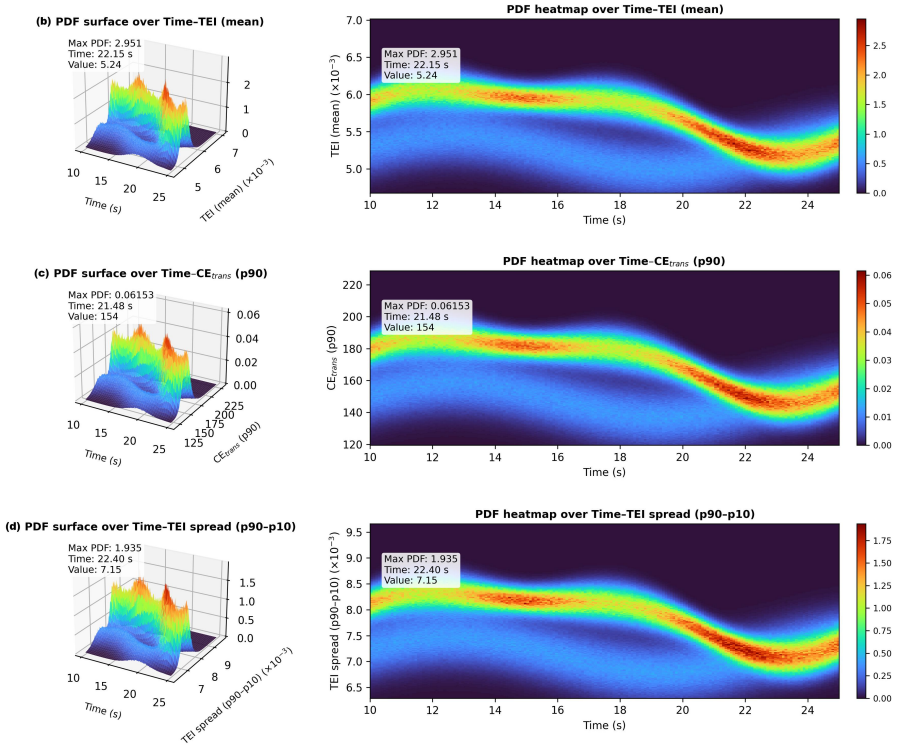

Figure 6. Time-evolving probability density of transportation impact metrics by truck class: TEI and CE_trans (3D PDF surfaces and heatmaps).

For example, when the sample was stratified by distance quartiles, the median transport emissions increased from approximately ~43 $kgCO_2e$ in the lowest distance quartile (≤~24 km one-way) to about ~132 $kgCO_2e$ in the highest quartile (≥~45 km one-way), a rise of roughly ~210%. Trip frequency showed an equally strong effect: the median transport footprint for deliveries requiring ≥4 round trips was nearly 3–4× the median for those delivered in a single round trip. These patterns justify treating distance and trip planning as first-order carbon drivers rather than secondary details.

The proposed Transportation Efficiency Index (TEI) was reported in **Figure 6** as $m^3/kgCO_2e$. For readability in narrative interpretation, TEI can also be expressed as $L/kgCO_2e$ (multiply by 1,000). In this dataset, TEI clustered around ~5–6 $L/kgCO_2e$ on average, with a wide spread between low-efficiency shipments (≈2–3 $L/kgCO_2e$) and high-efficiency shipments (≈10 $L/kgCO_2e$). Furthermore, when transport efficiency was normalized per distance and trip exposure, the median emissions-per-km metric improved by approximately ~13% between low and high load-factor quartiles—supporting the operational relevance of consolidation and payload utilization even when distance remains fixed.

Installation-stage inventories and emissions are summarized in **Figure 7**. Installation emissions were relatively stable compared with production and transport, averaging approximately 24–25 $kgCO_2e$ per component. This stability is consistent with installation being driven primarily by lifting cycles and site routines rather than highly variable material inputs; nevertheless, installation remains important because it can be influenced by delivery sequencing (reducing crane idle), standardized lift points, and coordinated scheduling.

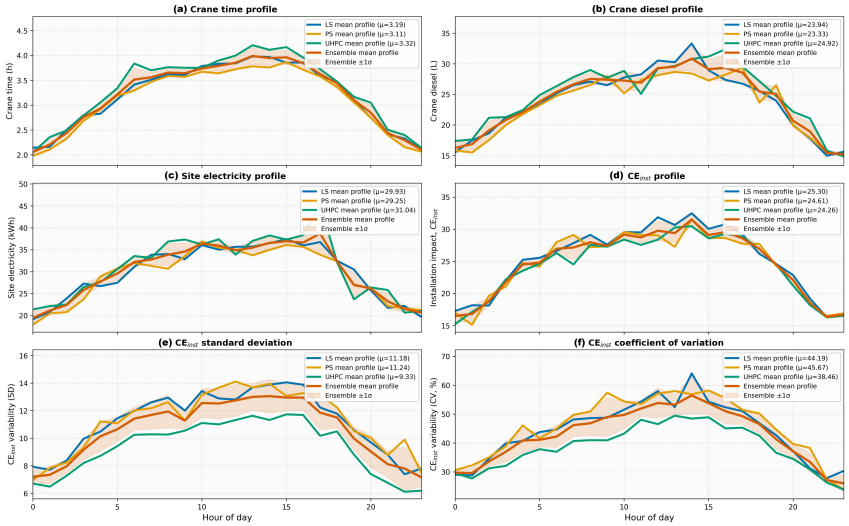

Figure 7. Component-type comparison of installation-stage activity and emissions: Load-curve profiles with variability (ensemble ±1σ, SD, and CV).

4.2. Predictive model performance and explainable drivers (ML + XAI)

4.2.1. Benchmark comparison across targets

To evaluate rapid prediction capability for decision support, multiple ML models were benchmarked against each other for three prediction targets: production emissions, transport emissions, and total cradle-to-site emissions. Performance metrics (R^2, RMSE, MAE, MAPE) are reported in **Figure 8**.

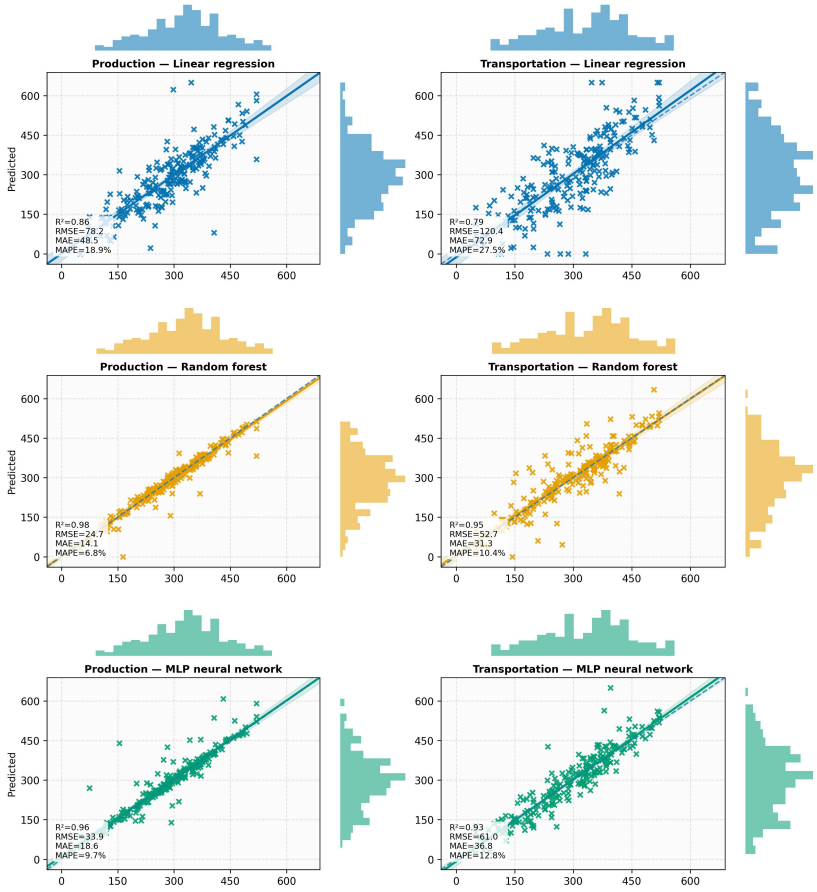

Figure 8. *Cont.*

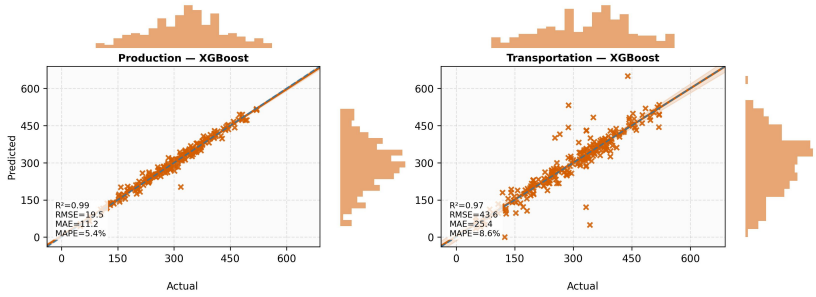

Figure 8. Model validation via actual–predicted joint plots: comparative performance of benchmark algorithms for production and transportation emissions.

Across all targets, gradient-boosted trees (XGBoost) delivered the best overall accuracy. For production emissions, XGBoost achieved near-ceiling performance ($R^2 \approx 0.99$, MAPE ≈ 5–6%), outperforming random forests and neural networks and substantially exceeding linear regression (**Figure 8**). For transportation emissions, accuracy remained high ($R^2 \approx 0.97$, MAPE < 9%) despite greater operational variability (distance, trips, truck class, and utilization). For total emissions, XGBoost again ranked first ($R^2 \approx 0.98$) and reduced error metrics relative to baseline models (**Figure 8**). The consistent uplift over linear regression supports the presence of non-linearities and interaction effects (e.g., volume × strength × CSR, distance × trips × truck class) that cannot be captured reliably by purely linear structures.

4.2.2. Explainability summary: What drives emissions and in which direction

Model explainability was reported using SHAP-based feature attribution to convert predictive gains into operational insight. The top drivers, ranked by normalized mean absolute SHAP magnitude, are listed in **Figure 9**.

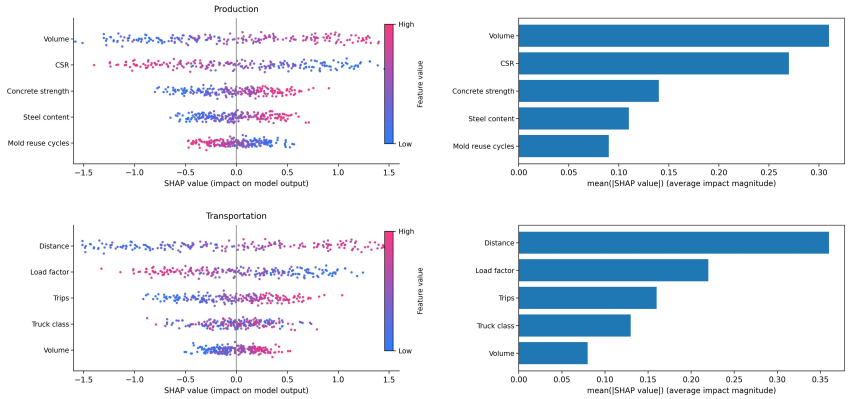

Figure 9. Explainability results for cradle-to-site emission prediction: SHAP summary plots and mean(|SHAP|) feature importance for two modeled targets.

For production, the most influential variables were volume (positive effect), CSR (negative effect), and material specification proxies (e.g., concrete strength and steel content, both positive). Mold reuse cycles showed a negative contribution, consistent with amortization: higher reuse lowered per-component mold burden (**Figure 9**). For transportation, the dominant drivers were distance (positive), load factor (negative), trips (positive), and truck class (mixed sign depending on operating regime). For installation, crane time and volume were the primary drivers, with crew hours and site electricity providing secondary contributions (**Figure 9**). This stage-specific

separation of drivers is essential for practice: it avoids the common pitfall of prescribing "one-size-fits-all" reductions and instead links each stage to its controllable levers. To further strengthen sensitivity interpretation, the analysis was also extended across the main modeling assumptions and operational variables. In particular, sensitivity was examined for material-related parameters (e.g., concrete class, steel-related inputs, and mold reuse effects) as well as logistics-related variables (e.g., distance, trip frequency, truck class, and payload utilization). This broader perspective complements the SHAP-based feature attribution by clarifying how variations in key assumptions influence stage-specific and total emissions outcomes.

To further examine non-linear relationships beyond individual feature importance, interaction effects among major predictors were also interpreted quantitatively. In particular, the combined influence of component volume and concrete specification on production emissions, as well as the interaction between transport distance, trip frequency, and load factor on transportation emissions, was examined through model response patterns and joint sensitivity interpretation. These interaction effects confirm that emissions do not change linearly with isolated parameters, but rather emerge from coupled operational conditions across design and logistics decisions.

A more comprehensive sensitivity perspective was also incorporated to clarify how the main controllable variables affect the results. In particular, SHAP-based explainability was used to quantify the relative influence and direction of key predictors, while scenario analysis was employed to examine how changes in standardization, mold reuse, load factor, trip frequency, and logistics coordination alter stage-specific and total emissions. In addition, the reported distributions and percentile-based comparisons help reflect uncertainty arising from operational variability rather than relying solely on average values.

4.3. Scenario outcomes and integrated mitigation evidence

To complement the model-based analysis, sensitivity to key assumptions was further examined through percentile-based comparisons and scenario testing. Variations in transportation distance, round-trip frequency, payload utilization, and standardization levels were analyzed to assess how operational changes influence carbon emissions across production, transportation, and installation stages. This additional layer of analysis improves the interpretability of the findings and reduces the risk of over-reliance on average-case assumptions.

To translate the empirical findings into decision-oriented evidence, four scenarios were evaluated: a baseline reflecting current operating averages, a design standardization scenario, a logistics optimization scenario, and an integrated scenario combining both. Relative results are reported in **Figure 10** as multipliers normalized to baseline (=1.00).

The design standardization scenario increased average CSR and mold reuse cycles and yielded a reduction in production emissions to roughly 0.90× baseline, producing a corresponding reduction in total emissions to approximately 0.92×. The logistics optimization scenario improved load factor and reduced trip exposure, lowering transport emissions to roughly 0.78× baseline and total emissions to around 0.90×.

The integrated scenario delivered the largest gains, lowering production and transport concurrently (≈0.88× and 0.75×, respectively) and reducing the total footprint to approximately 0.83× baseline, i.e., a ~17% total reduction (**Figure 10**). In TEI terms, these logistics changes correspond to an increase in transport efficiency on the order of ~25–30% under integrated planning, which is consistent with the strong influence of trip consolidation and payload utilization observed in the empirical distributions.

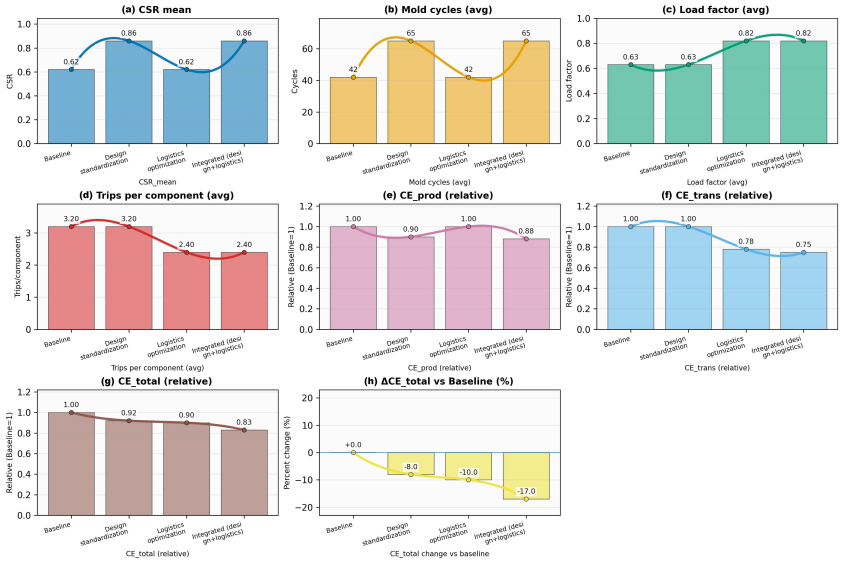

Figure 10. Comparative multi-metric performance of mitigation scenarios (relative to baseline).

Crucially, the scenario results show that carbon reduction is not confined to a single stage: meaningful mitigation emerges when standardized design families (enabling reuse and lower scrap) are aligned with carbon-aware logistics (reducing kilometers-per-delivered-volume and unnecessary trips). The scenario evidence therefore supports a coherent, stage-spanning mitigation logic that can be operationalized in procurement, production planning, and delivery scheduling.

In addition, a broader sensitivity perspective was incorporated to test the robustness of the main findings under variations in key assumptions. The sensitivity assessment focused on material-related parameters (e.g., concrete class and mold reuse effects), logistics-related variables (e.g., route distance, trip frequency, and payload utilization), and installation-related activity levels. The results consistently indicated that transportation efficiency variables and standardization-related production variables remained among the most influential drivers, thereby supporting the robustness of the principal conclusions.

5. Discussion

5.1. Key findings and interpretation of mechanisms

5.1.1. Overall pattern

The central message is that carbon mitigation for prefabricated buildings cannot be credibly managed by looking at factory production alone. The evidence from the three-stage accounting (production–transport–installation) showed that production

typically remained the largest contributor to cradle-to-site emissions, yet transportation frequently became the dominant marginal lever for specific deliveries because it was strongly shaped by controllable logistics variables (distance, trips, truck class, and load utilization). This aligns with the broader decarbonization challenge in buildings, where embodied and supply-chain decisions increasingly dominate early mitigation opportunities [108–110].

5.1.2. Why production was dominant

Production-stage dominance was consistent with the physics and chemistry of prefabricated concrete systems: cementitious materials and steel remain high-intensity inputs, and even efficient factories tend to exhibit relatively smaller direct-energy shares compared with upstream material burdens. Studies of prefabricated materialization stages similarly report that material production contributes the largest portion of emissions, often exceeding ~80% depending on scope and system boundaries [111].

5.1.3. Why transportation mattered more than "average factors" suggest

Transportation did not behave like a stable add-on; it behaved like a dispersion amplifier. Under otherwise similar component designs, transport emissions expanded rapidly with (i) longer routes, (ii) repeated trips driven by payload limits and scheduling constraints, and (iii) lower load factors. Prior logistics-focused research on prefabricated component delivery has emphasized that the "full-load rate" (load utilization) materially changes transportation emissions and should be treated explicitly rather than assumed constant [112–114].

Related transportation-planning research also shows that truck-capacity utilization and trip planning are central levers in prefabrication logistics (i.e., fewer trucks/trips through better consolidation and planning) [115–117].

5.1.4. Interpretation of TEI

The Transportation Efficiency Index (TEI) operationalized this variability by expressing delivered functional output per unit transport carbon (e.g., $m^3/kgCO_2e$). Conceptually, TEI behaved like a logistics "performance KPI" that captured multiple drivers simultaneously-distance, trip consolidation, and payload utilization-while remaining interpretable to planners. In practice, the TEI spread implied that carbon reductions were available without changing material design at all: consolidation, route rationalization, and improving load factors can move deliveries from the low-efficiency tail toward best practice, consistent with prior transportation-stage analyses for precast systems [118,119].

5.1.5. Why the ML+XAI results were plausible and decision-useful

The comparative performance of tree-based ensemble learning (notably XGBoost) was consistent with the structure of the problem: prefabricated carbon is driven by non-linearities and interactions (e.g., geometry × strength, distance × trips × truck class). XGBoost is specifically designed to capture such effects efficiently at scale [120]. The explainability layer (SHAP-based attribution) then translated predictive accuracy into actionable drivers, reducing the risk that the model functions as an opaque

"carbon oracle." SHAP's theoretical grounding and widespread adoption in high-stakes applications make it an appropriate choice for interpretable engineering analytics [121].

More broadly, interpretable ML and transparency are repeatedly emphasized as enabling conditions for trust, accountability, and adoption in high-stakes decision contexts [122, 123].

5.2. Comparison with previous studies and implications

5.2.1. Consistency with embodied-carbon literature

The finding that production/material inputs dominated most component footprints was directionally consistent with multiple prefabrication LCA studies, especially those framing the "materialization stage" as production + transport + site activities and reporting that upstream materials control the majority share [124–126]. The present results reinforced a more nuanced conclusion: while production tends to dominate the mean, transportation can dominate the variance, which is precisely what matters for targeted mitigation and robust procurement decisions.

5.2.2. Advancement beyond transportation as a fixed parameter

Many project-level assessments still model transportation using generic distance assumptions and fixed emission factors. In contrast, logistics-focused studies have shown that prefabricated delivery is structurally different from bulk material hauling because stacking limits, geometry constraints, and safety requirements reduce achievable load utilization; therefore, the transport footprint depends strongly on load rate and trip planning [127, 128]. By embedding TEI and explicitly predicting transportation emissions with ML + XAI, the study's framework operationalized these insights for early-stage decision support rather than treating transport as an afterthought.

Beyond the environmental dimension, the findings also have economic and long-term relevance. Improvements in transport efficiency, such as higher payload utilization, trip consolidation, and route rationalization, may reduce not only transport-related carbon emissions but also logistics-related operating costs. Likewise, greater design standardization and mold reuse can improve production repeatability and reduce resource inefficiencies over longer planning horizons. From a strategic perspective, these results suggest that the proposed framework can support not only short-term carbon reduction decisions but also longer-term industrial planning, procurement, and policy development for low-carbon prefabrication systems.

5.2.3. Implications for design and manufacturing strategy

The XAI results implied a clear separation of levers by stage. Production emissions were primarily sensitive to volume and material specification proxies, but they were also responsive to design-for-repeatability pathways (standardization, mold reuse, reduced rework, and scrap). Transportation emissions were more sensitive to logistics parameters than to component geometry alone, meaning that the same component design can carry materially different carbon outcomes depending on delivery planning. Practically, this supports an integrated "design + operations" strategy: standardize where structural and architectural constraints permit, then "lock

in" the carbon advantage by pairing standardized families with high-utilization logistics plans [129, 130]. These findings are also relevant from an economic perspective. Higher payload utilization, trip consolidation, and route rationalization can reduce not only transport-related carbon emissions but also fuel consumption, vehicle use intensity, and delivery-related operating costs. Likewise, greater design standardization and increased mold reuse may improve production repeatability, reduce waste, and lower per-unit manufacturing inefficiencies. Although a full cost-benefit assessment is beyond the scope of the present study, the results suggest that the proposed strategies are likely to support both environmental and operational efficiency.

In addition to environmental performance, the proposed framework also provides insights relevant to economic and operational scalability. Improvements in transportation efficiency (e.g., higher load factors, route consolidation, and reduced trip frequency) not only reduce carbon emissions but can also decrease logistics costs and improve supply chain productivity. Because the framework relies on operational data and interpretable machine-learning models, it can be scaled to other prefabrication plants or regional supply chains with similar datasets, supporting broader industrial applications and decision-making.

In addition to the environmental benefits, the results also have important economic implications. Improvements in logistics efficiency, including higher payload utilization, trip consolidation, and route rationalization, can reduce not only transport-related carbon emissions but also fuel consumption, vehicle use intensity, and delivery-related operating costs. Similarly, greater design standardization and higher mold reuse may improve production repeatability, reduce waste, and lower per-unit manufacturing inefficiencies. Although a full life-cycle cost assessment is beyond the present scope, the findings suggest that the proposed carbon-reduction strategies are also likely to support economic efficiency in prefabrication practice.

From an economic perspective, the proposed carbon-reduction strategies are closely aligned with cost-efficiency improvements. Logistics optimization measures such as higher payload utilization, reduced trip frequency, and route consolidation can directly decrease fuel consumption, transportation time, and fleet operating costs. Similarly, increased design standardization and mold reuse improve production efficiency by reducing setup time, material waste, and per-unit manufacturing costs. Although a full quantitative cost–benefit analysis is beyond the scope of this study, the results indicate a strong co-benefit relationship between carbon reduction and economic performance. Future work should integrate life-cycle cost analysis (LCCA) with the proposed framework to quantify these synergies more explicitly.

5.2.4. Implications for practitioners and policy

For industry, TEI offers a simple procurement-facing KPI that can be included in logistics contracts (e.g., minimum TEI targets by component class, reporting of load factors and trip counts). For policymakers and clients, the results support shifting embodied-carbon guidance from static checklists toward performance-based reporting that requires transparent transport assumptions and encourages consolidation and low-carbon fleets where feasible. This direction is consistent with the broader policy push to address building-sector emissions with better measurement and earlier

intervention in the value chain [131–133]. More specifically, the proposed framework supports a shift from simplified embodied-carbon reporting toward transparent, stage-integrated assessment of production, transportation, and installation emissions. In this context, the Transportation Efficiency Index (TEI) can serve as a practical benchmark for logistics-related carbon performance in procurement documents, contractor evaluation, and low-carbon reporting systems. Policymakers and public clients may also use such indicators to encourage higher transport efficiency, better load consolidation, and more standardized low-carbon prefabrication practices.

The results also have direct policy relevance. From a regulatory and procurement perspective, the proposed framework supports a shift from simplified embodied-carbon reporting toward more transparent, stage-integrated assessment of production, transportation, and installation emissions. In particular, the Transportation Efficiency Index (TEI) may serve as a practical benchmark for logistics-related carbon performance in contracts, reporting frameworks, and low-carbon procurement criteria. Policymakers and public clients may also use such indicators to encourage higher transport efficiency, better load consolidation, and more standardized low-carbon prefabrication practices.

For practical implementation, the framework can be applied in a stepwise manner. First, manufacturers can establish component-level carbon inventories using available production, shipment, and installation records. Second, predictive models can be used during design and planning stages to screen alternative component configurations and logistics strategies. Third, TEI and related operational indicators can be incorporated into delivery planning and contractor performance monitoring. In this way, the proposed framework is not limited to post hoc carbon accounting, but can function as a decision-support tool for day-to-day operational management and continuous improvement.

To strengthen the policy relevance of the findings, clearer regulatory and implementation pathways can be identified. Specifically, policymakers can integrate stage-wise carbon reporting (production–transport–installation) into building codes and environmental product declarations (EPDs). In addition, the proposed Transportation Efficiency Index (TEI) can be operationalized as a performance-based indicator in procurement regulations, requiring contractors to report load factors, trip frequency, and transport emissions. Governments and public clients may further encourage low-carbon prefabrication through incentives for high standardization rates, optimized logistics planning, and low-emission vehicle adoption. These measures provide a direct pathway from analytical results to enforceable regulatory frameworks.

5.2.5. Why explainability matters for adoption

In engineering domains, predictive accuracy alone rarely drives adoption; decision-makers must also understand "why" a recommendation is made, particularly when it affects cost, schedule, and safety. The XAI layer, therefore, served as more than visualization-it reduced deployment risk and supported accountable decision-making, echoing responsible-AI arguments in the explainability literature [134, 135].

5.2.6. Practical implementation examples

To facilitate industry adoption, several practical implementation examples can be derived from the proposed framework:

1. **Design stage:** Designers can use the predictive model to compare alternative component geometries and material specifications, selecting options with lower embodied carbon while maintaining structural requirements.
2. **Factory operations:** Manufacturers can increase the Component Standardization Rate (CSR) to enhance mold reuse cycles, thereby reducing production emissions and improving operational efficiency.
3. **Logistics planning:** Contractors can optimize delivery schedules by consolidating shipments, increasing load factors, and minimizing unnecessary trips, guided by TEI benchmarking.
4. **Procurement and contracting:** Clients can include TEI thresholds and carbon reporting requirements in contracts to ensure accountability and continuous improvement.

These examples demonstrate that the framework is not limited to analytical assessment but can be directly embedded into real-world decision-making processes across the prefabrication supply chain.

5.3. Strengths, limitations, future directions

5.3.1. Strengths

Three strengths are noteworthy. First, the framework treated the cradle-to-site boundary as a system (production–transport–installation), which is closer to how prefabrication decisions are actually made and aligns with "upfront/embodied carbon" framing in building decarbonization guidance [136–138]. Second, the introduction of TEI made transportation carbon interpretable and operationally measurable, consistent with logistics-focused work emphasizing explicit treatment of load utilization and transport planning [139, 140]. Third, the combination of ML with XAI addressed the accuracy–interpretability tension that often limits the practical uptake of data-driven decision tools in high-stakes settings [141, 142].

5.3.2. Limitations

Several limitations should be acknowledged more explicitly. First, the empirical analysis is based on a single regional case study, and therefore, the reported quantitative values may not be directly generalizable to other supply-chain, regulatory, or transport contexts. Second, while the study incorporates production, transportation, and installation stages, some operational variables, such as dynamic traffic conditions, backhauling, real-time fleet behavior, and detailed site disruptions, were not modeled explicitly. Third, the study emphasizes environmental performance, while economic feasibility was discussed qualitatively rather than through a full life-cycle cost framework. These limitations do not undermine the analytical contribution, but they define important directions for further validation and application.

Although the empirical framework was developed using a high-resolution dataset from a major prefabrication facility in Tehran, its methodological structure

is transferable to other plants and regional supply chains that maintain comparable production, logistics, and installation records. Nevertheless, broader validation across multiple factories, cities, and regulatory contexts is an important next step to confirm the generalizability of the reported driver rankings, TEI distributions, and scenario outcomes. This limitation has been acknowledged and highlighted as a priority for future research.

In addition, the empirical basis of the study reflects a single-facility, single-region case, and therefore the reported quantitative values should not be interpreted as universally representative of all prefabrication supply chains. Although the proposed framework is methodologically transferable, broader validation across multiple plants, cities, and regulatory contexts is necessary to confirm the generalizability of driver rankings, TEI distributions, and scenario outcomes.

Finally, while the study discusses economic relevance qualitatively, it does not include a full life-cycle cost framework or long-term financial evaluation. These limitations do not undermine the analytical contribution, but they define important directions for broader validation and future methodological extension.

5.3.3. Future research

Three extensions would strengthen both scientific contribution and transferability:

1. Multi-factory, multi-city datasets to test the robustness of TEI distributions and driver rankings across different fleet compositions and route structures.
2. Dynamic logistics modeling, integrating real-time constraints (traffic, time windows, and loading bay availability) and explicitly modeling backhauls and partial loads.
3. Optimization-linked decision support, where the interpretable predictor becomes a constraint or objective inside design and logistics optimization (e.g., jointly minimizing total kgCO_2e, cost, and schedule risk).
4. Future work should also incorporate explicit life-cycle cost considerations, longer-term operational planning horizons, and cross-regional industrial validation to further enhance the transferability and decision-making value of the proposed framework.
5. Future work should also incorporate explicit cost-benefit analysis, longer-term sustainability assessment, and multi-region empirical testing to further strengthen the transferability and real-world applicability of the proposed framework.
6. Future work should also include dedicated quantitative interaction analysis among major predictors, more extensive global sensitivity analysis, and explicit empirical modeling of transportation–installation coupling under dynamic site and logistics conditions.
7. Future research should expand the proposed framework through multi-region and multi-factory validation, explicit life-cycle cost assessment, and longer-term scenario analysis to further improve the practical transferability and decision-support value of the model.

5.3.4. Summary of the discussion

Overall, the discussion supports a clear conclusion: meaningful carbon reduction in prefabricated construction requires shifting from single-stage accounting to integrated, explainable, and operations-aware modeling. By quantifying and interpreting the drivers of production and transportation emissions simultaneously—and translating logistics performance into an interpretable TEI metric—the study strengthened the evidence base for actionable decarbonization at the component level, where early design and delivery decisions have outsized leverage [143–146].

Beyond immediate carbon reduction, the findings are relevant to long-term sustainability planning in prefabricated construction systems. Design standardization, reusable production assets, and coordinated logistics strategies can improve not only short-term carbon performance but also the long-term consistency, resilience, and resource efficiency of industrialized construction supply chains. From this perspective, the framework can support longer-term strategic planning for manufacturers, contractors, and policymakers seeking durable pathways toward low-carbon construction.

6. Conclusion

This study developed and demonstrated an integrated, cradle-to-site framework to quantify and predict carbon emissions across production, transportation, and installation for prefabricated building components using plant- and logistics-level operational data from a major facility in Tehran, Iran. The results showed that total cradle-to-site emissions averaged ≈ 591 $kgCO_2e$ per component (P10–P90 ≈ 260–1,064 $kgCO_2e$), highlighting substantial heterogeneity that cannot be captured by single "typical" factors. Production remained the dominant contributor on average (≈79% of total emissions), while transportation and installation accounted for ≈16% and ≈5%, respectively; however, transportation exhibited the strongest variability and became the key marginal lever for reduction in high-distance, low-utilization deliveries. In predictive terms, gradient-boosted models achieved high accuracy for emissions estimation (R^2 ≈ 0.99 for production, ≈0.97 for transportation, and ≈0.98 for total), enabling reliable screening of carbon outcomes during early planning. Explainable AI further revealed stage-specific drivers: volume and material specification proxies dominated production; distance, trip frequency, and load factor governed transportation; and crane time and volume shaped installation.

Scientifically, these findings advance prefabrication carbon research by moving beyond factory-only assessments and by operationalizing logistics impacts through a transparent Transportation Efficiency Index (TEI), which links emissions to delivered functional output and supports auditable decision-making. Practically, the framework provides manufacturers and contractors with actionable levers, standardizing component families to increase mold reuse and reduce production intensity, and optimizing routing, consolidation, and payload utilization to improve transport efficiency. Scenario evidence indicated that coordinated design and logistics

strategies can reduce total cradle-to-site emissions to roughly 0.83× baseline (≈17% reduction) while increasing transport efficiency (TEI) by ~25–30%. At the same time, the practical implementation of the framework requires attention to local logistics conditions, data availability, and operational constraints. Further multi-region validation and explicit economic assessment would strengthen its broader applicability.

Overall, the work underscores that credible decarbonization of prefabricated buildings requires simultaneous control of factory processes and logistics performance, not isolated optimization of either stage. The study is limited by its single-region operational context and simplified installation inventories. Future research should validate TEI and driver rankings across multiple cities and plants, incorporate dynamic routing and telematics-based fuel measurement, and embed the interpretable predictors into a multi-objective optimization that jointly considers carbon, cost, and schedule risk. These contributions establish a replicable foundation for stage-integrated, explainable carbon management in industrialized construction. At the same time, broader multi-region validation, explicit economic assessment, and further implementation-oriented testing would strengthen the wider applicability of the framework. These directions represent important next steps for translating the proposed approach into broader industrial and policy practice.

This study contributes to the growing body of knowledge on embodied carbon reduction in prefabricated construction by introducing an integrated, explainable, and operationally grounded framework. Beyond methodological advancements, the findings demonstrate that meaningful carbon reduction requires coordinated action across design, manufacturing, and logistics stages rather than isolated interventions. The proposed TEI metric, combined with explainable machine learning, provides a practical bridge between carbon accounting and actionable decision-making.

More broadly, the study highlights that prefabrication can serve as a scalable pathway toward low-carbon construction when supported by standardized design, efficient logistics, and data-driven planning. The framework also offers significant potential for integration into policy instruments, procurement strategies, and industrial practices. By linking environmental performance with operational efficiency and economic feasibility, this work contributes to advancing both scientific understanding and real-world implementation of sustainable prefabrication systems.

Author contributions: Conceptualization, PN, AN and FSGF (Farazin Soltani Gerd Faramarzi); methodology, PN, AN and FSGF (Faraneh Soltani Gerd Faramarzi); software, PN and AN; validation, PN, AN, TB and HG; formal analysis, PN, AN, TB and HG; investigation, PN, AN and FSGF (Faraneh Soltani Gerd Faramarzi); resources, PN, AN and FSGF (Farazin Soltani Gerd Faramarzi); data curation, PN and AN; writing—original draft preparation, PN and AN; writing—review and editing, PN, AN, TB, HG, FSGF (Faraneh Soltani Gerd Faramarzi) and FSGF (Farazin Soltani Gerd Faramarzi); visualization, PN and AN; supervision, PN and AN; project administration, PN and AN; funding acquisition, PN. All authors have read and agreed to the published version of the manuscript.

Funding: This work received no external funding.

Institutional review board statement: Not applicable.

Informed consent statement: Not applicable.

Data availability statement: Data will be made available on request.

Conflict of interest: The authors declare that they have no known competing financial interests or personal relationships that could have appeared to influence the work reported in this paper.

AI use statement: During the preparation of this manuscript, the authors used ChatGPT (OpenAI) solely for language refinement. No AI tools were used for data analysis, interpretation, or generation of scientific content. All outputs were critically reviewed and edited by the authors. The authors take full responsibility for the integrity and accuracy of the work.

Abbreviation

A4	Transport to site (life-cycle module A4)
A5	Construction/installation stage (life-cycle module A5)
AI	Artificial intelligence
ANN	Artificial neural network
BIM	Building information modeling
BOM	Bill of materials
C30	Concrete strength class C30
C35	Concrete strength class C35
C40	Concrete strength class C40
CDF	Cumulative distribution function
CE	Carbon emissions (stage-wise and total)
CO_2	Carbon dioxide
CSR	Component Standardization Rate
CV	Coefficient of variation
EF	Emission factor
EN	European Norm (standard)
I-01	Installation batch/type code (example record)
I-02	Installation batch/type code (example record)
I-03	Installation batch/type code (example record)
ID	Identifier
ISO	International Organization for Standardization
KPI	Key performance indicator
LCA	Life cycle assessment
LS	Component category label: LS (not expanded in manuscript)
MAE	Mean absolute error
MAPE	Mean absolute percentage error
ML	Machine learning
MLP	Multilayer perceptron (neural network)

MLR	Multiple linear regression
P1	1st percentile (used for outlier trimming)
P10	10th percentile
P90	90th percentile
P99	99th percentile (used for outlier trimming)
PDF	Probability density function
PS	Component category label: PS (not expanded in manuscript)
PVC	Polyvinyl chloride
QC	Quality control
R2	Coefficient of determination (R^2)
RMSE	Root mean square error
S-001	Shipment ID code (example record)
S-002	Shipment ID code (example record)
S-003	Shipment ID code (example record)
S-004	Shipment ID code (example record)
SD	Standard deviation
SHAP	SHapley Additive exPlanations
TEI	Transportation Efficiency Index
UHPC	Ultra-high-performance concrete
XAI	Explainable artificial intelligence
XG	Extreme gradient boosting (XGBoost)
XPS	Extruded polystyrene

References

1. Kim H, Kim S, Lee J, et al. Development of a blockchain-based platform for real-time carbon emission assessment of building material supply chain. Building and Environment. 2026; 287: 113907. doi: 10.1016/j.buildenv.2025.113907
2. Alaux N, Marton C, Steinmann J, et al. Whole-life greenhouse gas emission reduction and removal strategies for buildings: Impacts and diffusion potentials across EU Member States. Journal of Environmental Management. 2024; 370: 122915. doi: 10.1016/j.jenvman.2024.122915
3. Dos Santos BV, Da Silva Rêgo JH. A stochastic LCA model for estimating greenhouse gas emissions from federal highway construction projects in Brazil. Environmental Impact Assessment Review. 2025; 112: 107801. doi: 10.1016/j.eiar.2024.107801
4. Chen X, Huang M, Bai Y, et al. Sustainability of underground infrastructure—Part 1: Digitalisation-based carbon assessment and baseline for TBM tunnelling. Tunnelling and Underground Space Technology. 2024; 148: 105776. doi: 10.1016/j.tust.2024.105776
5. Klumbyte E, Georgali PZ, Spudys P, et al. Enhancing whole building life cycle assessment through building information modelling: Principles and best practices. Energy and Buildings. 2023; 296: 113401. doi: 10.1016/j.enbuild.2023.113401
6. Wang H, Zhang H, Zhao L, et al. Real-world carbon emissions evaluation for prefabricated component transportation by battery electric vehicles. Energy Reports. 2022; 8: 8186–8199. doi: 10.1016/j.egyr.2022.06.039
7. Xiao S, Fomin NI, Liu C, et al. Systematic review of high-performance grouting materials for prefabricated grouted sleeve connections in building structures. Results in Engineering. 2026; 29: 108505. doi: 10.1016/j.rineng.2025.108505
8. Zhang Y, Wang J, Long Z, et al. Temperature prediction and intelligent voltage regulation for direct electric curing of

concrete: Machine learning and experimental validation. Construction and Building Materials. 2025; 494: 143422. doi: 10.1016/j.conbuildmat.2025.143422
9. Naghipour P. Metaheuristic model tuning for energy forecasting in low-income housing in the MollaZeynal region of Tabriz city: Linking comfort and carbon. Next Research. 2026; 4: 101265. doi: 10.1016/j.nexres.2025.101265
10. Naghipour P, Naghipour A. Evaluating heating energy consumption in residential buildings using hybrid machine learning models: The case of Parsabad city. Next Research. 2025; 2(3): 100721. doi: 10.1016/j.nexres.2025.100721
11. Bringiotti A, Pallonetto F, De Rosa M. A demand-side optimisation framework for assessing energy flexibility potential of integrated energy systems in building complex. Applied Energy. 2026; 402: 127038. doi: 10.1016/j.apenergy.2025.127038
12. Naghipour P, Naghipour A. Energy performance analysis of residential buildings in Bandar Anzali: Influence of orientation and aspect ratio. Next Sustainability. 2025; 5: 100140. doi: 10.1016/j.nxsust.2025.100140
13. Osuizugbo IC, Orekan AA, Omer MM, et al. An exploratory factor analysis on technological-related barriers to the construction of zero-energy buildings in Nigeria. International Journal of Building Pathology and Adaptation. 2025; 43(7): 1897–1918. doi: 10.1108/IJBPA-05-2024-0091
14. Cheng S, Lin J, Xu W, et al. Carbon, water, land and material footprints of China's high-speed railway construction. Transportation Research Part D: Transport and Environment. 2020; 82: 102314. doi: 10.1016/j.trd.2020.102314
15. Lin B, Zheng L. Is the policy of massive transportation infrastructure construction hindering China's carbon reduction? Transportation Research Part A: Policy and Practice. 2026; 204: 104817. doi: 10.1016/j.tra.2025.104817
16. Alali AA, Huang Y, Tsavdaridis KD. Comparative life cycle assessment (LCA) of the composite prefabricated ultra-shallow slabs (PUSS) and hollow core slabs in the UK. Journal of Building Engineering. 2024; 96: 110588. doi: 10.1016/j.jobe.2024.110588
17. Gao H, Wang D, Du X, et al. An LCA-BIM integrated model for carbon-emission calculation of prefabricated buildings. Renewable and Sustainable Energy Reviews. 2024; 203: 114775. doi: 10.1016/j.rser.2024.114775
18. Ng C, Li M, Zhong RY, et al. Establishing carbon footprints for modular integrated construction logistics using cyber-physical internet routers. Transportation Research Part D: Transport and Environment. 2024; 133: 104259. doi: 10.1016/j.trd.2024.104259
19. Wang J, Li Xiao, Teng Y, et al. How to allocate carbon responsibility among stakeholders in the prefabricated construction supply chain? From a game theory perspective. Sustainable Cities and Society. 2026; 136: 107034. doi: 10.1016/j.scs.2025.107034
20. Yang S, Zhang W, Wu S, et al. Carbon emissions from express logistics: Estimation and spatial analysis using origin-destination transportation flows. Transport Policy. 2025; 171: 970–985. doi: 10.1016/j.tranpol.2025.07.002
21. Asadpour F, Hossein Shirdel A, Naghipour P. Evaluation of perceptual indicators of physical environment affecting the inducement of citizen's sense of place in urban neighborhoods. Energy and Buildings. 2024; 325: 114992. doi: 10.1016/j.enbuild.2024.114992
22. Gu X, Fan L, Mahabir R. Building carbon emissions (2016–2025): A PRISMA-based systematic review of definitions, quantification methods and policies. Environmental Development. 2026; 57: 101345. doi: 10.1016/j.envdev.2025.101345
23. Xu J, Shi Y, Xie Y, et al. A BIM-Based construction and demolition waste information management system for greenhouse gas quantification and reduction. Journal of Cleaner Production. 2019; 229: 308–324. doi: 10.1016/j.jclepro.2019.04.158
24. Abdullah AM, Zakoworotny M, Zhang C, et al. Rapid out-of-oven lamination (ROL) for energy-efficient manufacturing of carbon fiber reinforced composites. Composites Part A: Applied Science and Manufacturing. 2025; 194: 108873. doi: 10.1016/j.compositesa.2025.108873
25. Kodagali K, Rad CV, Sockalingam S, et al. Low-velocity impact response of hybrid pseudo-woven carbon/epoxy thin composite laminates manufactured via automated fiber placement. Materials Today Communications. 2026; 50: 114505. doi: 10.1016/j.mtcomm.2025.114505
26. Naghipour P, Naghipour A, Shirdel AH, et al. Sustainability in Historical Islamic Architecture: Lessons from Sheikh Lotfollah Mosque's Construction Techniques. Journal of Islamic Architecture. 2025; 8(3): 585–603. doi: 10.18860/jia.v8i3.29053
27. Sandanayake M, Gunasekara C, Law D, et al. Greenhouse gas emissions of different fly ash based geopolymer concretes in building construction. Journal of Cleaner Production. 2018; 204: 399–408. doi: 10.1016/j.jclepro.2018.08.311
28. Zhang L, Dong M. Assessment of CO_2 emissions in large-span, heavy-load buildings: A comparative study of

multi-ribbed concrete composite slabs and traditional cast-in-place concrete slabs. Journal of Cleaner Production. 2025; 521: 146187. doi: 10.1016/j.jclepro.2025.146187
29. Zhao Z, Mao J, Liu J, et al. Low-carbon electric curing of alkali-activated slag precast concrete: Advancing efficiency, energy savings, and carbon reduction. Journal of Building Engineering. 2025; 114: 114350. doi: 10.1016/j.jobe.2025.114350
30. Ma C. Sustainable manufacturing production synergy and circular economy model under low carbon energy based on thermal energy cycle and blockchain technology. Thermal Science and Engineering Progress. 2024; 55: 102944. doi: 10.1016/j.tsep.2024.102944
31. Machin Ferrero LM, Aráoz ME, Robles NL. Life cycle assessment of furfural production from sugarcane bagasse within a circular biorefinery framework. Biomass and Bioenergy. 2026; 208: 108878. doi: 10.1016/j.biombioe.2025.108878
32. Al-Ghussain L, Lu Z, Alrbai M, et al. Global techno-economic and life cycle greenhouse gas emissions assessment of solar and wind based renewable hydrogen production. Applied Energy. 2025; 401: 126595. doi: 10.1016/j.apenergy.2025.126595
33. Gozali L, Liu KV, Adianto A, et al. Greenhouse gas emission forecasting analysis in Jakarta towards net zero emissions in 2050. Case Studies in Chemical and Environmental Engineering. 2026; 13: 101315. doi: 10.1016/j.cscee.2025.101315
34. Sangeetha A, Amudha T. A Novel Bio-Inspired Framework for CO2 Emission Forecast in India. Procedia Computer Science. 2018; 125: 367–375. doi: 10.1016/j.procs.2017.12.048
35. Liu Q, Ma Y, Chen L, et al. Artificial intelligence for production, operations and logistics management in modular construction industry: A systematic literature review. Information Fusion. 2024; 109: 102423. doi: 10.1016/j.inffus.2024.102423
36. Wang H, Zhang H, Liu P. Adopting modular integrated construction (MiC) in road pavement construction: Concepts, applications, and challenges. Automation in Construction. 2026; 181: 106620. doi: 10.1016/j.autcon.2025.106620
37. Greer F, Horvath A. Modular construction's capacity to reduce embodied carbon emissions in California's housing sector. Building and Environment. 2023; 240: 110432. doi: 10.1016/j.buildenv.2023.110432
38. Li CZ, Tam VWy, Ma M, et al. Carbon emission analysis and multi-objective optimization of modular integrated construction using Petri net simulation. Energy and Buildings. 2025; 339: 115784. doi: 10.1016/j.enbuild.2025.115784
39. Mawra K, Rashid K, Alqahtani FK, et al. Sustainability assessment integrating BIM and decision-making for modular slab construction against conventional cast-in-situ. Engineering Science and Technology, an International Journal. 2024; 60: 101891. doi: 10.1016/j.jestch.2024.101891
40. Chen S, Chen K, Wu F, et al. Life cycle greenhouse gas emission of pork production in China: Carbon inequality embodied in supply chain. Resources, Conservation and Recycling. 2025; 220: 108386. doi: 10.1016/j.resconrec.2025.108386
41. Zou J, Xu H, Lan C, et al. Regulation of photoassimilate transportation and nitrogen uptake to decrease greenhouse gas emissions in ratooning rice with higher economic return by optimized nitrogen supplies. Field Crops Research. 2024; 312: 109385. doi: 10.1016/j.fcr.2024.109385
42. Chen J, Zhao F, Liu Z, et al. Greenhouse gas emissions from road construction in China: A province-level analysis. Journal of Cleaner Production. 2017; 168: 1039–1047. doi: 10.1016/j.jclepro.2017.08.243
43. Qu L, Cui Y, Huang G, et al. Greenhouse gas emissions from construction machinery in China: Historical trends and prospective reduction pathways. Journal of Environmental Sciences. 2025; S1001074225006096. doi: 10.1016/j.jes.2025.09.037
44. Ubolsook P, Podong C, Sedpho S, et al. Assessing the environmental impact of construction waste management in northern Thailand: An approach to estimate greenhouse gas emissions and cumulative energy demand. Journal of Cleaner Production. 2024; 467: 142961. doi: 10.1016/j.jclepro.2024.142961
45. Liu Y, Li J, Li M, et al. Better prediction of the carbon emissions from bridge construction: Machine learning methods and design parameters. Structures. 2025; 82: 110581. doi: 10.1016/j.istruc.2025.110581
46. Martínez A, Fan J, Miller SA. Machine learning in life cycle assessment and low carbon material discovery: Challenges and pathways forward for the construction industry. Resources, Conservation and Recycling. 2026; 224: 108567. doi: 10.1016/j.resconrec.2025.108567
47. Song Q, Xu S, Lu Y, et al. Study on the characteristics and prediction of concrete carbon emissions based on a machine learning approach with spatiotemporal heterogeneity analysis. Case Studies in Construction Materials.

2025; 23: e05410. doi: 10.1016/j.cscm.2025.e05410
48. Gong P, Xu X, Ma Z, et al. Strength characteristics, microstructure, and carbon footprint assessment of backfill materials based on multi-source coal-based solid wastes. Environmental Research. 2026; 288: 123214. doi: 10.1016/j.envres.2025.123214
49. Miao H, Wang P, Wu J, et al. Highly efficient and broad-spectrum antibacterial carbon dots combat antibiotic resistance. Talanta. 2025; 281: 126926. doi: 10.1016/j.talanta.2024.126926
50. Alves JL, Palha RP, Almeida Filho ATD. Towards an integrative framework for BIM and artificial intelligence capabilities in smart architecture, engineering, construction, and operations projects. Automation in Construction. 2025; 174: 106168. doi: 10.1016/j.autcon.2025.106168
51. Farahzadi L, Kioumarsi M. Application of machine learning initiatives and intelligent perspectives for CO_2 emissions reduction in construction. Journal of Cleaner Production. 2023; 384: 135504. doi: 10.1016/j.jclepro.2022.135504
52. Garlet L, Bracht MK, Lamberts R, et al. Artificial intelligence to enhance BIM-BEPS integration via IFC: Challenges, solutions, and future directions. Advanced Engineering Informatics. 2026; 69: 103824. doi: 10.1016/j.aei.2025.103824
53. Sivashanmugam S, Rodriguez Trejo S, Rahimian F. BIM-integrated semantic framework for construction waste quantification and optimisation. Automation in Construction. 2024; 168: 105842. doi: 10.1016/j.autcon.2024.105842
54. Allana S, Dara R, Lin X, et al. Towards integration of privacy enhancing technologies in explainable artificial intelligence. Knowledge-Based Systems. 2026; 335: 115235. doi: 10.1016/j.knosys.2025.115235
55. Konhäuser K, Werner T. Uncovering the financial impact of energy-efficient building characteristics with eXplainable artificial intelligence. Applied Energy. 2024; 374: 123960. doi: 10.1016/j.apenergy.2024.123960
56. Mustaffa Z, Sulaiman MH. Advanced forecasting of building energy loads with XGBoost and metaheuristic algorithms integration. Energy Storage and Saving. 2025; 4(4): 421–438. doi: 10.1016/j.enss.2025.03.005
57. Naghipour P, Naghipour A, Bakirova T, et al. Adobe versus concrete: Passive energy analysis in residential buildings in the hot and arid climate of Kashan city. Building Engineering. 2026; 4(1). doi: 10.59400/be4029
58. Bibri SE, Huang J. AI and AI-powered digital twins for smart, green, and zero-energy buildings: A systematic review of leading-edge solutions for advancing environmental sustainability goals. Environmental Science and Ecotechnology. 2025; 28: 100628. doi: 10.1016/j.ese.2025.100628
59. Ma Y, Shi Y, Gao M, et al. XAI driven analysis of multidimensional sustainability factors: Evidence from TFP of Chinese listed companies. Applied Soft Computing. 2026; 188: 114486. doi: 10.1016/j.asoc.2025.114486
60. Wu Y, Li Y, Zheng Z, et al. Assessing structural behavior of prefabricated volumetric building modules during transportation. Thin-Walled Structures. 2026; 218: 114165. doi: 10.1016/j.tws.2025.114165
61. Yin Y, Yu Q, Zhang Y, et al. Deflection monitoring of immersed tunnel element during floating transportation and installation based on series camera network. Optics and Lasers in Engineering. 2024; 172: 107857. doi: 10.1016/j.optlaseng.2023.107857
62. Zhang Y, Ma T, Yang H. Prediction-based optimal system design of an improved building-to-vehicle-to-building energy community under different operation strategies concerning three PV installation types. Energy. 2025; 341: 139439. doi: 10.1016/j.energy.2025.139439
63. Cai J, Zhao Z, Zhou Z, et al. Predicting the carbon emission reduction potential of shared electric bicycle travel. Transportation Research Part D: Transport and Environment. 2024; 129: 104107. doi: 10.1016/j.trd.2024.104107
64. Jaller M, Xiao R, Dennis-Bauer S, et al. Estimating last-mile deliveries and shopping travel emissions by 2050. Transportation Research Part D: Transport and Environment. 2023; 123: 103913. doi: 10.1016/j.trd.2023.103913
65. Jang J, Sung M, Hwang J. When less travel means more carbon: How rainfall-induced shifts from public transit to cars increase urban transport emissions. Science of The Total Environment. 2026; 1013: 181269. doi: 10.1016/j.scitotenv.2025.181269
66. Li S, Li SL, Xu S, et al. Assessing the potential for traffic carbon emission reductions through residential travel mode shifts: insights from massive vehicle trajectory data and scenario simulations. International Journal of Applied Earth Observation and Geoinformation. 2025; 142: 104684. doi: 10.1016/j.jag.2025.104684
67. Lei W, Aldlemy MS, Falah MW, et al. Adaptive deep meta-learning ensembles for robust daily carbon emission forecasting in major continent economies. Journal of Cleaner Production. 2025; 530: 146804. doi: 10.1016/j.jclepro.2025.146804
68. Ramarope SI, Fatoba OS, Jen TC. Hydro-power generation forecast in South Africa based on Machine Learning

(ML) models. Scientific African. 2023; 22: e01981. doi: 10.1016/j.sciaf.2023.e01981
69. Shahbazbegian A, Ghiasi M. Developing a machine learning (ML) based graphical user interface (GUI) for significant wave height (SWH) forecasting to support wave energy converters (WECs) operations planning. Renewable Energy. 2026; 256: 124490. doi: 10.1016/j.renene.2025.124490
70. Hou ZW, Di QB, Chen XL. Forecasting carbon emissions in Chinese coastal cities based on a gated recurrent unit model. Energy Reports. 2024; 12: 5747–5756. doi: 10.1016/j.egyr.2024.11.048
71. Liu Y, Luo W, Tang X, et al. Integrating STIRPAT: Adaboost and data-driven for influencing factors analysis and scenario prediction of carbon emission during building materialization stage. Urban Climate. 2025; 62: 102555. doi: 10.1016/j.uclim.2025.102555
72. Olfert V, Yang K, Rochel P, et al. Predictive modeling of tolerance-dependent failure behavior of self-pierce riveted joints: From coupon-level tests to sub-component validation. Journal of Manufacturing Processes. 2026; 157: 1250–1273. doi: 10.1016/j.jmapro.2025.12.058
73. Wang Z, Yang X, Zhan Z, et al. Carbon emission measurement and evaluation of large public buildings in the materialization stage. Energy and Buildings. 2024; 324: 114840. doi: 10.1016/j.enbuild.2024.114840
74. Li S, Lou B, Hu G, et al. Quantifying CO_2 hydrate sequestration: a multi-physics simulation of megatonne-scale transport and millennial-scale trapping dynamics. Fuel. 2026; 408: 137680. doi: 10.1016/j.fuel.2025.137680
75. Zhang Y, Huang L, Wang J, et al. Data-driven optimization for maritime logistics: integrating transport network mining with ship fleet routing. Transportation Research Part C: Emerging Technologies. 2026; 183: 105451. doi: 10.1016/j.trc.2025.105451
76. Famiglini L, Campagner A, Barandas M, et al. Evidence-based XAI: An empirical approach to design more effective and explainable decision support systems. Computers in Biology and Medicine. 2024; 170: 108042. doi: 10.1016/j.compbiomed.2024.108042
77. Yang Y, Zheng B, Luk C, et al. Towards a sustainable circular economy: Understanding the environmental credits and loads of reusing modular building components from a multi-use cycle perspective. Sustainable Production and Consumption. 2024; 46: 543–558. doi: 10.1016/j.spc.2024.02.027
78. Bayley T, Ward T, Sturman F, et al. ML-ABC: Machine-learning assisted Approximate Bayesian Computation for efficient calibration of agent-based models for pandemic outbreak analysis. Epidemics. 2026; 54: 100881. doi: 10.1016/j.epidem.2025.100881
79. Becker I, Anderson F, Phillips AR. Structural design of hybrid steel-timber buildings for lower production stage embodied carbon emissions. Journal of Building Engineering. 2023; 76: 107053. doi: 10.1016/j.jobe.2023.107053
80. Zheng Y, Havu M, Liu H, et al. Direct CO_2 emissions and uptake at neighbourhood-scale across the urban area of Beijing. City and Environment Interactions. 2025; 28: 100252. doi: 10.1016/j.cacint.2025.100252
81. Jalaei F, Guest G, Gaur A, et al. Exploring the effects that a non-stationary climate and dynamic electricity grid mix have on whole building life cycle assessment: A multi-city comparison. Sustainable Cities and Society. 2020; 61: 102294. doi: 10.1016/j.scs.2020.102294
82. Skiles MJ, Kassel D, King CW, et al. Effect of building sector retrofits on natural gas demand and electricity supply during winter weather emergencies. Results in Engineering. 2026; 29: 108509. doi: 10.1016/j.rineng.2025.108509
83. Lü X, Lu W. Building output–input function of catalytic combustion sensor to diesel vapor. Measurement. 2010; 43(4): 596–602. doi: 10.1016/j.measurement.2010.01.003
84. Liu H, Yao Y, Chen Z, et al. Grey water reuse of a multi-functional super-high building: evaluation of model treatment processes. Desalination and Water Treatment. 2018; 116: 96–102. doi: 10.5004/dwt.2018.22608
85. Kunkatla CK, Namburu SK. A relative analysis of standard labour output constants for building construction works and materials in Andhra Pradesh state, India. Materials Today: Proceedings. 2022; 60: 1588–1595. doi: 10.1016/j.matpr.2021.12.124
86. Wang W, Osaragi T. Lognormal distribution of daily travel time and a utility model for its emergence. Transportation Research Part A: Policy and Practice. 2024; 183: 104058. doi: 10.1016/j.tra.2024.104058
87. Luo N, Nara A, Khoo HL, et al. An integration modeling framework for individual-scale daily mobility estimation. Travel Behaviour and Society. 2024; 34: 100650. doi: 10.1016/j.tbs.2023.100650
88. Cornette JFP, Blondeau J. Operational greenhouse gas emissions of various energy carriers for building heating. Cleaner Energy Systems. 2024; 9: 100148. doi: 10.1016/j.cles.2024.100148
89. Fallahi Z, Plewe K, Smith AD. Energy-related emissions from commercial buildings: Comparing methods for quantifying temporal indirect emissions associated with electricity purchases. Sustainable Energy Technologies and Assessments. 2018; 30: 150–163. doi: 10.1016/j.seta.2018.09.004

90. Hao M, Li Y, Chen X, et al. Optimization design method of C30/C40 fly ash concrete based on machine learning and elite retention genetic algorithm. Advances in Engineering Software. 2025; 210: 104019. doi: 10.1016/j.advengsoft.2025.104019
91. Nguyen QT, Sağıroğlu S, Livaoğlu R. Effects of concrete-to-concrete surface treatment methods on the bending behavior of RC buildings: A numerical investigation. Structures. 2025; 80: 110099. doi: 10.1016/j.istruc.2025.110099
92. Feng H, Zhang Y, Xin H, et al. Restrained Shrinkage in Ultra-High-Performance Concrete (UHPC)-Normal strength concrete interface. Journal of Building Engineering. 2025; 111: 113293. doi: 10.1016/j.jobe.2025.113293
93. Li J, Zhu S, Li GQ, et al. Preventing fire-induced brittle collapse of steel tubular space trusses for reliable early warning: From mechanisms to design strategy. Fire Safety Journal. 2026; 159: 104586. doi: 10.1016/j.firesaf.2025.104586
94. Han TV, MoonSook J, Kim Y, et al. Experimental and analytical studies on the compressive behaviors of a 3D-printed sand mold-cast S-CN connector in modular steel buildings. Alexandria Engineering Journal. 2026; 134: 473–493. doi: 10.1016/j.aej.2025.12.013
95. Kongkatigumjorn N, Crespy D. Strategies to prepare polymers with cleavable linkages releasing active agents in acidic media. Polymer Chemistry. 2024; 15(44): 4491–4518. doi: 10.1039/D4PY00854E
96. Gingrich S, Matej S, Erb KH, et al. An option space approach to wood use: Providing structural timber for buildings while safeguarding forest integrity. iScience. 2025; 28(10): 113472. doi: 10.1016/j.isci.2025.113472
97. Astrain D, Pascual N, Catalán L, et al. Continuous electric energy production in Antarctica through Geothermal Passive Thermoelectric Generators. Applied Thermal Engineering. 2025; 279: 127517. doi: 10.1016/j.applthermaleng.2025.127517
98. Kytinou VK, Metaxa ZS, Zapris AG, et al. Exploitation of extruded polystyrene (XPS) waste for lightweight, thermal insulation and rehabilitation building applications. Developments in the Built Environment. 2024; 20: 100580. doi: 10.1016/j.dibe.2024.100580
99. Martínez JS, Gallego D, Ojeda S. JH. Theoretical determination of electronic properties of resorcinol and hydroquinone as building blocks of molecular wires. RSC Advances. 2025; 15(52): 44194–44204. doi: 10.1039/D5RA06041A
100. Martinez L, Klitou T, Olschewski D, et al. Advancing building intelligence: Developing and implementing standardized Smart Readiness Indicator (SRI) on-site audit procedure. Energy. 2025; 316: 134538. doi: 10.1016/j.energy.2025.134538
101. Hatami-Marbini A, Babaei A, Akbari Jokar MR. Optimising inventory management and collaborative supply chains: A robust data envelopment analysis-based approach. European Journal of Operational Research. 2026; 331(3): 894–915. doi: 10.1016/j.ejor.2025.10.016
102. Hassen AY, Arashpour M, Abdi E. Lightweight segmentation model for automated facade installation in high-rise buildings. Advanced Engineering Informatics. 2025; 65: 103374. doi: 10.1016/j.aei.2025.103374
103. Kaspersen B, Lohne J, Bohne RA. Exploring the CO_2-Impact for Building Height: A Study on Technical Building Installations. Energy Procedia. 2016; 96: 5–16. doi: 10.1016/j.egypro.2016.09.089
104. Wu P, Low SP, Jin X. Identification of non-value adding (NVA) activities in precast concrete installation sites to achieve low-carbon installation. Resources, Conservation and Recycling. 2013; 81: 60–70. doi: 10.1016/j.resconrec.2013.09.013
105. Mossberg A, Wetterqvist C, Holmstedt L, et al. A methodology for the integration of fire risk in building life cycle analysis. Fire Safety Journal. 2026; 160: 104601. doi: 10.1016/j.firesaf.2025.104601
106. Naghipour P, Naghipour A, Bakirova T. Life-cycle assessment and multi-objective optimization of natural-insulated envelopes across Iranian climates. Building Engineering. 2026; 4(1). doi: 10.59400/be3952
107. Ukwaththa J, Herath S, Meddage DPP. A review of machine learning (ML) and explainable artificial intelligence (XAI) methods in additive manufacturing (3D Printing). Materials Today Communications. 2024; 41: 110294. doi: 10.1016/j.mtcomm.2024.110294
108. Jha NK, Lohani SP, Khatiwada D, et al. Assessing greenhouse gas emissions and decarbonization potential of household biogas plant: Nepal's case study. Energy for Sustainable Development. 2024; 83: 101592. doi: 10.1016/j.esd.2024.101592
109. Li H, Shen G, Senemmar S, et al. Real-time greenhouse gas emission intensity informed demand-side load regulation for power grid decarbonization. Cell Reports Sustainability. 2025; 2(5): 100367. doi: 10.1016/j.crsus.2025.100367
110. Mebarki C, Tidadini AMBA, Derradji L, et al. Assessing the economic, environmental, and energy

impacts of natural gas-powered VRF system for building sector decarbonization: An integrated all-in-one package methodology based on open BIM approach. Building and Environment. 2026; 290: 114201. doi: 10.1016/j.buildenv.2026.114201
111. Kang ST, Park JH, Yuk H, et al. Advanced Trombe wall façade design for improving energy efficiency and greenhouse gas emissions in solar limited buildings. Solar Energy. 2025; 293: 113492. doi: 10.1016/j.solener.2025.113492
112. Chang CC, Chang KC, Lin YL. Policies for reducing the greenhouse gas emissions generated by the road transportation sector in Taiwan. Energy Policy. 2024; 191: 114171. doi: 10.1016/j.enpol.2024.114171
113. Di Lullo G, Giwa T, Okunlola A, et al. Large-scale long-distance land-based hydrogen transportation systems: A comparative techno-economic and greenhouse gas emission assessment. International Journal of Hydrogen Energy. 2022; 47(83): 35293–35319. doi: 10.1016/j.ijhydene.2022.08.131
114. Melikoglu M. Türkiye's transportation sector's greenhouse gas emissions: Multimodal forecasting and analysis. Next Research. 2025; 2(4): 101070. doi: 10.1016/j.nexres.2025.101070
115. Jiao T, Peng P, Li S, et al. Low-carbon efforts for underground space development in Singapore. Underground Space. 2026; 26: 22–35. doi: 10.1016/j.undsp.2025.07.004
116. Ma J, Cao J, Benedetti L, et al. Environmental and economic optimization of relocation strategies for mobile prefabrication factories in infrastructure projects. Developments in the Built Environment. 2025; 24: 100744. doi: 10.1016/j.dibe.2025.100744
117. Zhai Y, Zhong RY, Huang GQ. Towards Operational Hedging for Logistics Uncertainty Management in Prefabrication Construction. IFAC-PapersOnLine. 2015; 48(3): 1128–1133. doi: 10.1016/j.ifacol.2015.06.235
118. Qu H, Dong W, Li Z, et al. Performance evaluation of prefabricated retaining wall systems based on centrifuge tests. Proceedings of the Institution of Civil Engineers - Engineering Sustainability. 2024; 1–20. doi: 10.1680/jensu.23.00072
119. Xiong W, Baccay MA. Economic benefits of adopting prefabricated building systems in the Philippines. KSCE Journal of Civil Engineering. 2025; 29(12): 100282. doi: 10.1016/j.kscej.2025.100282
120. Yan H, He Z, Gao C, et al. Investment estimation of prefabricated concrete buildings based on XGBoost machine learning algorithm. Advanced Engineering Informatics. 2022; 54: 101789. doi: 10.1016/j.aei.2022.101789
121. Zhou C, Wang Z, Wang X, et al. Deciphering the nonlinear and synergistic role of building energy variables in shaping carbon emissions: A LightGBM- SHAP framework in office buildings. Building and Environment. 2024; 266: 112035. doi: 10.1016/j.buildenv.2024.112035
122. Ertosun Yıldız M, Beyhan F. Prediction of cooling load via machine learning on building envelope design parameters. Journal of Building Engineering. 2025; 100: 111724. doi: 10.1016/j.jobe.2024.111724
123. Zhou D, Jia Y, Zhang N, et al. An ensemble machine-learning model with online learning strategy for building load forecasting. Applied Thermal Engineering. 2026; 288: 129434. doi: 10.1016/j.applthermaleng.2025.129434
124. Ferrández D, Zaragoza-Benzal A, Velilla JPD, et al. Towards a more sustainable construction: A multi-criteria evaluation of prefabricated block technologies. Resources, Conservation & Recycling Advances. 2026; 29: 200301. doi: 10.1016/j.rcradv.2025.200301
125. Ma X, Huang M, Chen X, et al. BIM-integrated LCA framework for prefabricated buildings with automated benchmarking and visual decision support. Building and Environment. 2025; 286: 113689. doi: 10.1016/j.buildenv.2025.113689
126. Xu A, Zhu Y, Wang Z, et al. Carbon emission calculation of prefabricated concrete composite slabs during the production and construction stages. Journal of Building Engineering. 2023; 80: 107936. doi: 10.1016/j.jobe.2023.107936
127. Parlikar A, Tepe B, Möller M, et al. Quantifying the carbon footprint of energy storage applications with an energy system simulation framework — Energy System Network. Energy Conversion and Management. 2024; 304: 118208. doi: 10.1016/j.enconman.2024.118208
128. Solgi H, Rezaei F, Burg V, et al. Carbon footprint analysis of non-fossil heating strategies for agricultural greenhouses in Switzerland. Energy Conversion and Management: X. 2025; 28: 101304. doi: 10.1016/j.ecmx.2025.101304
129. Abdelghany MB, Dan M, Al-Durra A, et al. Unified control architecture for resilient hydrogen mobility with heterogeneous storage under realistic market logistics delays. Applied Energy. 2026; 403: 127066. doi: 10.1016/j.apenergy.2025.127066
130. Chen SY, Song Y, Albright D, et al. Logistics planning for direct temporary disaster housing assistance under demand

uncertainty. Socio-Economic Planning Sciences. 2024; 96: 102072. doi: 10.1016/j.seps.2024.102072
131. Maierhofer D, Van Karsbergen V, Potrč Obrecht T, et al. Linking forest carbon opportunity costs and greenhouse gas emission substitution effects of wooden buildings: The climate optimum concept. Sustainable Production and Consumption. 2024; 51: 612–627. doi: 10.1016/j.spc.2024.08.021
132. Saleh Saleh MA, AlShafeey M. Recurrent neural network strategies for decoupling energy consumption and greenhouse gas emissions in Hungary's industrial sector. Energy Conversion and Management: X. 2025; 28: 101219. doi: 10.1016/j.ecmx.2025.101219
133. Tsai WT, Tsai CH. Interactive Analysis of Green Building Materials Promotion With Relevance to Energy Consumption and Greenhouse Gas Emission. In: Comprehensive Green Materials. Elsevier; 2025. pp. 200–219. doi: 10.1016/B978-0-443-15738-7.00050-7
134. Rasel MA, Abdul Kareem S, Kwan Z, et al. Bluish veil detection and lesion classification using custom deep learnable layers with explainable artificial intelligence (XAI). Computers in Biology and Medicine. 2024; 178: 108758. doi: 10.1016/j.compbiomed.2024.108758
135. Yuan L, Gu Y, Han Y, et al. Exploring transparency in pathological image analysis: A comprehensive review of explainable artificial intelligence (XAI) techniques. Computer Science Review. 2026; 60: 100863. doi: 10.1016/j.cosrev.2025.100863
136. Alam M, Rakib AKM, Hasan ASMM, et al. Decarbonizing road transportation: Barriers and drivers in an emerging economy context. Transportation Research Part D: Transport and Environment. 2025; 143: 104723. doi: 10.1016/j.trd.2025.104723
137. Li Y, Pittau F, Masera G. Global embodied carbon in buildings: Meta-analysis and science-based decarbonization through technological solutions. Journal of Building Engineering. 2026; 117: 114909. doi: 10.1016/j.jobe.2025.114909
138. Yang L, Ma S, Chen X, et al. The impact of emerging intercity travel modes on transportation decarbonization. Transport Policy. 2025; 173: 103794. doi: 10.1016/j.tranpol.2025.103794
139. Cui H, Lu Y, Zhou Y, et al. Carbon flow through continental-scale ground logistics transportation. iScience. 2023; 26(1): 105792. doi: 10.1016/j.isci.2022.105792
140. Neu W, Eschment L, Napier J, et al. Next Generation Logistics CargoTube: Carbon Neutral High Throughput Logistics By Low-pressure Tube Transportation. Transportation Research Procedia. 2023; 72: 2944–2951. doi: 10.1016/j.trpro.2023.11.841
141. Haghighat M, MohammadiSavadkoohi E, Shafiabady N. Applications of Explainable Artificial Intelligence (XAI) and interpretable Artificial Intelligence (AI) in smart buildings and energy savings in buildings: A systematic review. Journal of Building Engineering. 2025; 107: 112542. doi: 10.1016/j.jobe.2025.112542
142. Khan MA, Farooq MS, Saleem M, et al. Smart buildings: Federated learning-driven secure, transparent and smart energy management system using XAI. Energy Reports. 2025; 13: 2066–2081. doi: 10.1016/j.egyr.2025.01.063
143. Carmona-Martínez AA, Rueda A, Jarauta-Córdoba CA. Deep decarbonization of the energy intensive manufacturing industry through the bioconversion of its carbon emissions to fuels. Fuel. 2024; 371: 131922. doi: 10.1016/j.fuel.2024.131922
144. Li Ziyi, Li Junjie, Wang X, et al. Decarbonizing photovoltaic glass manufacturing in China: A factory-specific carbon footprint analysis. Environmental Technology & Innovation. 2025; 40: 104669. doi: 10.1016/j.eti.2025.104669
145. Ten KH, Kang HS, Siow CL, et al. Automatic identification system in accelerating decarbonization of maritime transportation: The state-of-the-art and opportunities. Ocean Engineering. 2023; 289: 116232. doi: 10.1016/j.oceaneng.2023.116232
146. Zhou Y, Dong Q, Som H, et al. Sustainable environmental design using circular economy in the plastic manufacturing industry for decarbonization. Computers & Industrial Engineering. 2026; 213: 111764. doi: 10.1016/j.cie.2025.111764